UCRL-16345

University of California

Ernest O. Lawrence Radiation Laboratory

STATISTICAL MODEL CALCULATIONS OF HIGH ENERGY REACTIONS

TWO-WEEK LOAN COPY

This is a Library Circulating Copy
which may be borrowed for two weeks.
For a personal retention copy, call
Tech. Info. Division, Ext. 5545

Berkeley, California

DISCLAIMER

This document was prepared as an account of work sponsored by the United States Government. While this document is believed to contain correct information, neither the United States Government nor any agency thereof, nor the Regents of the University of California, nor any of their employees, makes any warranty, express or implied, or assumes any legal responsibility for the accuracy, completeness, or usefulness of any information, apparatus, product, or process disclosed, or represents that its use would not infringe privately owned rights. Reference herein to any specific commercial product, process, or service by its trade name, trademark, manufacturer, or otherwise, does not necessarily constitute or imply its endorsement, recommendation, or favoring by the United States Government or any agency thereof, or the Regents of the University of California. The views and opinions of authors expressed herein do not necessarily state or reflect those of the United States Government or any agency thereof or the Regents of the University of California.

Research and Development UCRL-16315

UNIVERSITY OF CALIFORNIA
Lawrence Radiation Laboratory
Berkeley, California

AEC Contract No. W-7405-eng-48

STATISTICAL MODEL CALCULATIONS OF HIGH ENERGY REACTIONS

Graham H. Campbell
(Ph. D. Thesis)

August 10, 1965

STATISTICAL MODEL CALCULATIONS OF HIGH ENERGY REACTIONS

Graham H. Campbell

Lawrence Radiation Laboratory
University of California
Berkeley, California

August 10, 1965

ABSTRACT

Calculations based on a covariant version of the Fermi statistical model have been made in an attempt to fit the known gross features of elementary particle reactions at energies presently accessible to accelerators. Our aim was to provide an extrapolation of these data to the higher energies of future accelerators. The n-fold phase space integration required for the model was reduced to a single contour integral which was approximated by a saddle point technique. Resonance states were included as final state particles. The initial predictions of this model were not in agreement with experiments and although modifications of the model were found to improve the situation we show that none of these modifications yield a reliable method of extrapolation to higher energy.

I. INTRODUCTION

Multiple production processes in elementary particle physics are notoriously intractable within any known theoretical framework. Fermi has proposed a model for high energy interactions based on the idea that the statistical weight of a given final state should provide a first approximation to the relative probability of this state.[1] Calculations based on a relativistic version of this model were undertaken with the hope that they might provide a simple background for discussion of elementary particle interactions at the energies now accessible to accelerators and a means for making estimates for the next generation of accelerators. Unfortunately the results of this investigation have been predominately negative. The straight forward predictions of this model at currently available energies are not in agreement with experience although there are numerous ways to improve the model there is no unique way in which this may be done. Thus this model cannot provide a simple background for more refined calculations. The value of the model for extrapolation in energy is destroyed by its asymptotic behavior which does not agree with cosmic ray data and is also hampered by the non-uniqueness of the fit to accelerator data. Thus with this model we can approximate known results but are unable to predict new ones.

The phase space model on which our calculations are based is discussed in Section II. In Section III it will be shown that the phase space integrations can be reduced to a single integral, and in

Section IV we will indicate how this integral is approximated and consider the accuracy of the approximation. The description of the calculation is completed in Section V where the method by which isotopic spin coupling coefficients are computed is discussed. We present the method by which predictions of particle spectra are determined in Section VI and compare the predictions of the model to experimental data in Section VII. Section VIII contains our conclusions.

II. THE PHASE SPACE MODEL

The phase space or "statistical" model has been "justified" in many ways since Fermi's original, appealingly intuitive, approach. The following argument is made from a view point close to that of Hagedorn.[2]

If we characterize the final states by the linear momenta and masses of the particles they contain then the cross section from a given initial state is proportional to:[3]

$$\sigma_f \sim \int |F_f|^2 \, \delta^{(4)}(P - \sum_i p_i) \prod_i \theta(p_i^{\,o}) \, \delta(p_i^{\,2} - m_i^{\,2}) \times (2m_i) \frac{d^3 p_i}{(2\pi)^3} \tag{1}$$

where F_f is the invariant amplitude, P is the total 4-momenta of the initial state and the index i runs over final state particles.

The conservation laws of strong interactions enable us to determine (or approximate) the dependence of F_f on some of the final state variables. The additive conservation laws of baryon number and strangeness are imposed by allowing only final states consistent with the conservation of these quantities.

Isotopic spin can be conserved by considering initial states of pure isotopic spin, characterizing final states by the isotopic spin of their constituents and using the projection operator upon the final state defined by

$$P_T \, |t_i \, , \, \theta_i\rangle = \Gamma_{t_i \theta_i}^{\;\;T} \, |T, \sum_i \theta_i\rangle \tag{2}$$

where T is total isotopic spin, t_1 and θ_i are total and third-component of isospin for the final state particles. The calculation of the numerical factors $\Gamma_{t_i \theta_i}{}^{T}$ will be discussed in Section V.

The conservation of angular momentum could, in principle, be taken into account by using projection operators in a similar manner,[4] however this is quite impractical for extensive calculations.[5] Thus we shall take into account the spin multiplicity of final states by inserting a factor

$$\prod_i (2 s_i + 1) \tag{3}$$

and neglect conservation of total angular momentum. This has been shown to introduce an error of about 10% .[4]

If we now recognize the essential equivalence of part of our problem with the traditional counting of states problem, we can approximate two other dependences of the amplitude. The influence of statistics may be approximated by eliminating double counting of equivalent states in the integration over momenta. This gives a factor

$$\prod_j \frac{1}{n_j!} \tag{4}$$

where n_j is the number of identical particles of the jth type. Furthermore, if we calculate the density of states in a box we get a factor of V^{n-1} where V is the volume of the box and n is the number

of particles. Removal of this factor leaves an amplitude whose dimensions no longer depend upon the number of final state particles.

We now remove the amplitude from the integral using the mean-value theorem yielding

$$\sigma_f \sim \overline{|F_f|^2}\, V^{n-1} \frac{\prod_i (2s_i + 1)}{\prod_j n_j\,!} \left(\Gamma_{t_i \theta_i}{}^T\right)^2 S_n(P, m_i) \tag{5}$$

where

$$\begin{aligned} S_n(P, m_i) &= \int \delta^{(4)}(P - \sum_i p_i) \prod_i \frac{d^3 p_i}{\omega_i} \frac{m_i}{(2\pi)^3} \\ \omega_i &= \sqrt{\vec{p}_i^{\,2} + m_i^2} \quad . \end{aligned} \tag{6}$$

As Hagedorn emphasizes, everything to this point is rigorous (all knowledge lies in $\overline{F}_f$) and the phase space model predicts only average values. It is <u>not</u> in conflict with anisotropic angular distributions.

However now we must cover up our lack of knowledge by making drastic approximations to $|\overline{F}_f|^2$. First, we can approximately account for one of the predominate features of high energy physics, the occurance of resonances. We do this by a method due to Belenki and Nikishov[6] and justified by Belenky,[7] which simply includes the resonances as final state particles which decay after leaving the primary reaction. Second, if we consider the inverse process of the final state particles in a box coming together to form the initial state, then

the interchange of the summing over final states and the averaging over initial states indicates that this cross section is proportional to $\overline{|F|^2}$. This, for purely geometrical reasons, contains a factor of $\left(\frac{\Omega}{V}\right)^{n-1}$ where Ω is the volume in which the particles interact.[8] We now insert this, which amounts to replacing V by Ω. Since we interpret Ω as an interaction volume and yet wish to allow for different ranges of interaction we make the replacement

$$\Omega^{n-1} \longrightarrow \prod_i v_i \tag{7}$$

where the v_i are individual interaction volumes (these v_i are the parameters of the model). Now we have inserted an extra dimensioned quantity (a volume) so we no longer have a cross section, but since we shall give up hope of an absolute normalization we shall interpret this quantity as the unnormalized relative probability of the final state f.

The factors v_i are expected to be of the order of magnitude of a sphere of radius equal to the range of interaction. We shall take

$$v_i = \xi_i \frac{4}{3}\pi \frac{1}{\mu_i^3} \tag{8}$$

where μ_i is the pion mass for non-strange particles and the mass of the K - meson for strange particles. The ξ_i are the parameters actually used in the calculations.

Now the third and most presumptous approximation is that the remainder of $\overline{|F_f|^2}$ is a constant and hence may be ignored, since it will cancel upon normalization. This approximation, although necessary to yield a model upon which simple calculations can be based, has many more or less obvious short comings. The physical picture of this model, as embodied in our consideration of the inverse process, is that of two particles colliding and forming a "hot spot" which reaches a thermal equilibrium and from which all final states are equally accessible on an á priori basis

In view of recent information on the peripheral nature of these reactions it is clear that this is far too simple a picture and probably not even a good approximation to average properties of the collisions.

Another short coming is in the treatment of spin. A correct treatment of spin would introduce energy dependent factors in the integrand (e.g. this is why the non-covariant form of the phase space is appropriate in studying the end point of β - decay spectra, a relativistic process). A more appropriate approach would probably be to apply the above type argument to the Stapp M-functions[9] which have simple analyticity properties and hence are better approximated by slowly varying functions in the physical region. This would separate explicitly the energy dependent factors due to spin,[10] but one is left with various spin α indices to be contracted in an unknown manner . This destroys the value of such an approach.

III. REDUCTION OF THE INTEGRAL

We are faced with the problem of computing

$$S_n(P,m_i) = \int \delta^{(4)} \left(P - \sum_{i=1}^{n} p_i\right) \prod_{i=1}^{n} \frac{d^3p_i}{\omega_i} \quad . \tag{9}$$

This is a Lorentz invariant quantity and we will show that in the center of mass frame it may be reduced to a single (contour) integral that may be well approximated by the saddle-point technique.

If we insert a Fourier representation of the δ-function we may write

$$S_n(E,m_i) = \frac{1}{(2\pi)^4} \int_{-\infty-i\epsilon}^{\infty-i\epsilon} d\alpha\, e^{i\alpha E} \int d^3\lambda \prod_{i=1}^{n} \int \frac{d^3p_i}{\omega_i}\, e^{i(\vec{\lambda}\cdot\vec{p}_i - \alpha\omega_i)} \tag{10}$$

where we have given the variable α a small imaginary part to make the integration over momenta well defined.[11]

Now consider

$$J(\vec{\lambda},\alpha,m) = \int \frac{d^3p}{\omega}\, e^{i(\vec{\lambda}\cdot\vec{p} - \alpha\omega)} \quad . \tag{11}$$

Then

$$J = \frac{2\pi}{i\lambda} \int_{-\infty}^{\infty} \frac{p\,dp}{\omega} \; e^{i(\lambda p - \alpha\,\omega)}$$

$$= -\frac{2\pi}{\lambda} \frac{d}{d\lambda} \int_{-\infty}^{\infty} \frac{dp}{\omega} \; e^{i(\lambda p - \alpha\,\omega)} \qquad (12)$$

$$= -\frac{2\pi}{\lambda} \frac{d}{d\lambda} \; I(\lambda, \alpha, m)$$

where $\lambda = |\vec{\lambda}|$ and $p = |\vec{p}|$. If we now let

$$p = m \sinh \theta$$

$$\omega = m \cosh \theta$$

$$\alpha = \sqrt{\alpha^2 - \lambda^2} \; \cosh \psi \qquad (13)$$

$$\lambda = \sqrt{\alpha^2 - \lambda^2} \; \sinh \psi$$

then

$$I(\lambda, \alpha, m) = \int_{-\infty}^{\infty} d\theta \; e^{-im\sqrt{\alpha^2 - \lambda^2} \; \cosh(\theta - \psi)}$$

$$= \int_{-\infty}^{\infty} d\varphi \; e^{-im\sqrt{\alpha^2 - \lambda^2} \; \cosh \varphi} \qquad (14)$$

$$= -i\,\Pi\, H_0^{(2)} \left(m\sqrt{\alpha^2 - \lambda^2} \right) .$$

The last equality follows from an integral representation for the Hankel function of the second kind.[12] The negative imaginary part of α defines the square root with the convention that the square root becomes real and positive as α becomes real and greater than λ. Differentiating with respect to λ, we find

$$J(\vec{\lambda},\alpha,m) = \frac{2\pi^2 \, im}{\sqrt{\alpha^2 - \lambda^2}} \; H_1^{(2)}\left(m\sqrt{\alpha^2 - \lambda^2}\right) . \qquad (15)$$

The angular integrations for S_n are trivial and we have

$$S_n(E,m_i) = \frac{4\pi}{(2\pi)^4} \int_{-\infty - i\epsilon}^{\infty - i\epsilon} d\alpha \int_0^{\infty} d\lambda \, \lambda^2 \, E^{i\alpha E} \; f\left(\sqrt{\alpha^2 - \lambda^2}\right) \qquad (16)$$

where

$$f\left(\sqrt{\alpha^2 - \lambda^2}\right) = \prod_{k=1}^{n} \left[\frac{2\pi^2 \, i \, m_k}{\sqrt{\alpha^2 - \lambda^2}} \; H_1^{(2)}\left(m_k\sqrt{\alpha^2 - \lambda^2}\right)\right] . \qquad (17)$$

Two comments upon this equation are in order. First, the sole role of ϵ is to define the continuation of the square root, since except for this the expression is independent of ϵ. Second, if we examine this form before the angular integrations are done, and using an arbitrary Lorentz frame, we notice that it is just a Fourier transformation in a space with a time-like dimension. Thus, the following steps seem to be a generalization of a theorem of Bochner's on Fourier transformations of radial functions.[13]

In order to perform an additional quadrature, we shall replace the α integration by an integration over $\rho = \sqrt{\alpha^2 - \lambda^2}$. This will necessitate a separate consideration of different domains of integration. We shall write

$$S_n(E, m_i) = \frac{4\pi}{(2\pi)^4} \left\{ \int_0^R d\lambda \int_{C_1} d\alpha + \int_R^\infty d\lambda \int_{C_2} d\alpha \right\} \lambda^2 e^{i\alpha E} f\left(\sqrt{\alpha^2 - \lambda^2}\right) \tag{18}$$

where the contours C_1 and C_2 are those defined in Figures 1 and 2 respectively. For convenience, the parts of the contours indicated as circular arcs will actually be taken to be those shapes leading to circular arcs in the variable ρ . We shall denote the contributions to S_n from the various labeled portions of the α contours simply by those labels. Consider, as an example, the calculation of S_I ,

$$S_I = \int_R^\infty d\lambda \int_{-\infty}^{-\sqrt{\lambda^2 + R^2}} d\alpha \; \lambda^2 \; e^{i\alpha E} \; f\left(\sqrt{\alpha^2 - \lambda^2}\right) \tag{19}$$

make the change of variable defined by

$$\begin{aligned} \rho &= \sqrt{\alpha^2 - \lambda^2} = -r \; ; \; r > 0 \\ \alpha &= \sqrt{\rho^2 + \lambda^2} = -\sqrt{r^2 + \lambda^2} \end{aligned} \tag{20}$$

then,

$$S_I = \int_R^\infty d\lambda \int_{-\infty}^{-R} d\rho \; \frac{\rho \lambda^2}{-\sqrt{\lambda^2 + r^2}} \; e^{-iE\sqrt{\lambda^2 + r^2}} \; f(\rho) \tag{21}$$

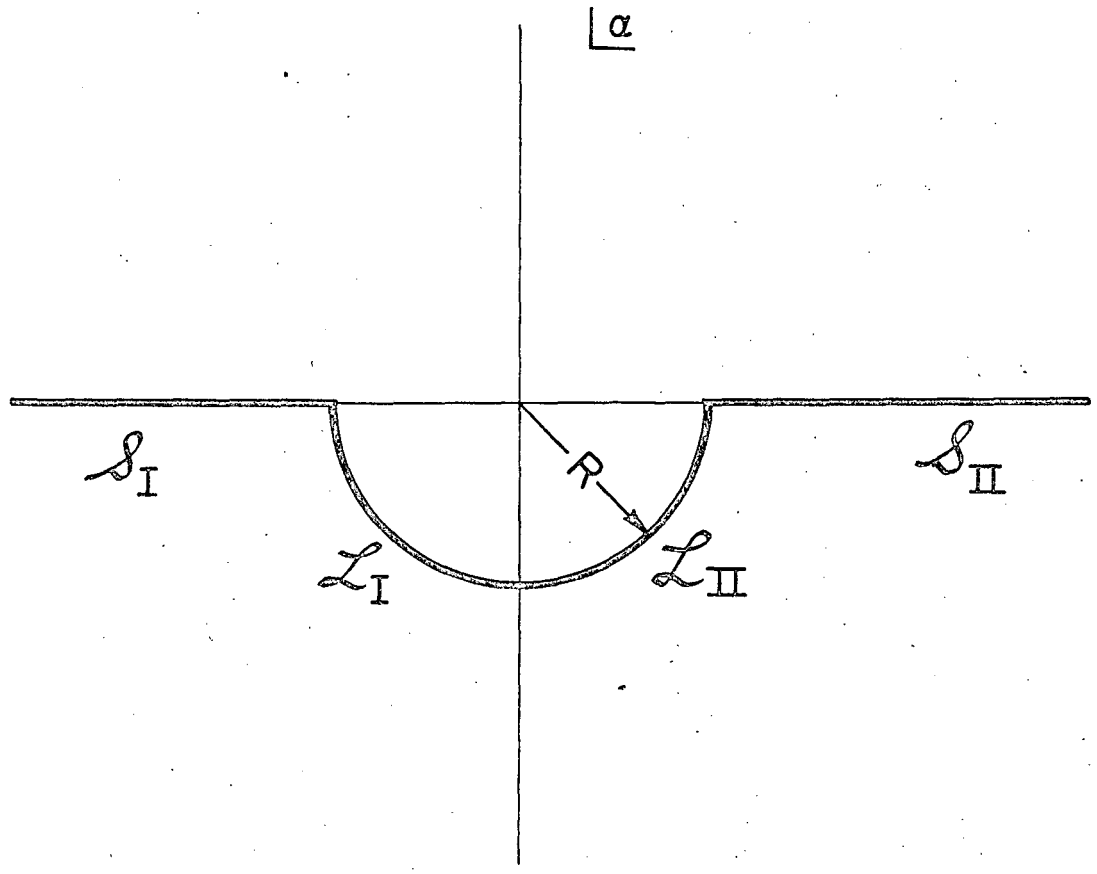

MU-36509

Fig. 1. Integration contour in α - plane for $|\lambda| < R$.

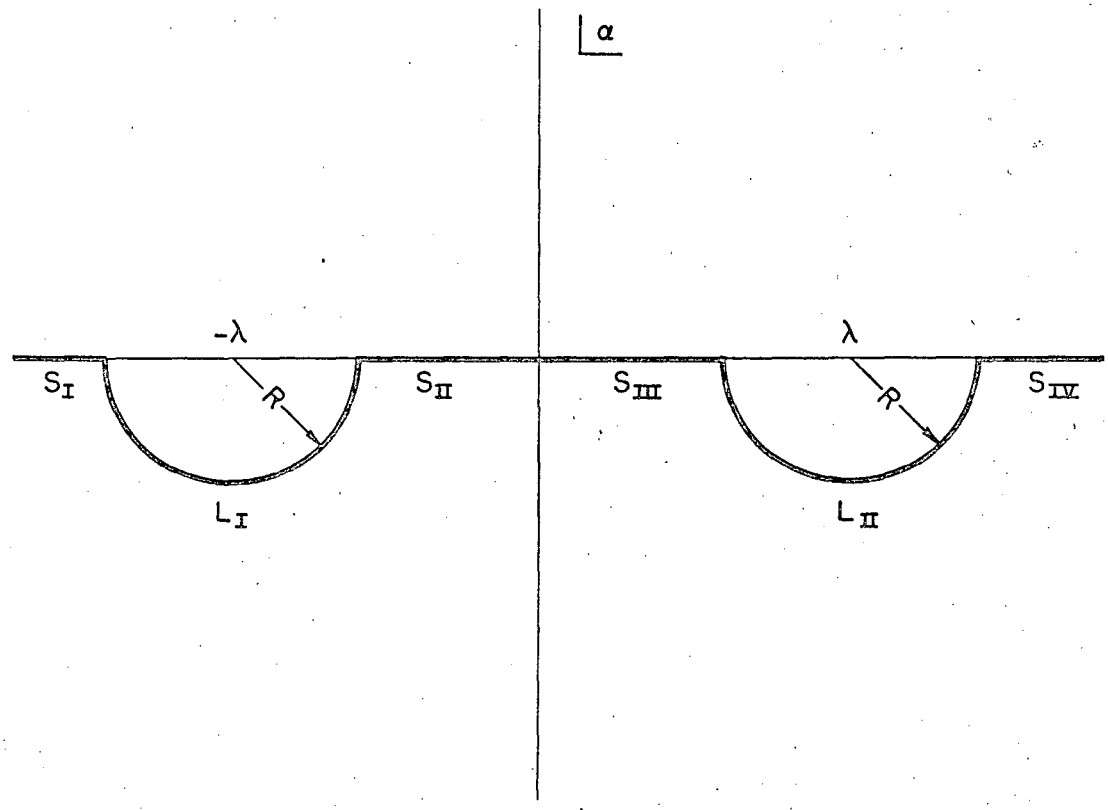

MU-36510

Fig. 2. Integration contour in α - plane for $|\lambda| > R$.

where the phase of ρ is $-\pi$. The order of integration can now be reversed. For $\mathcal{L}_I$ we make the same change of variable. This yields

$$\mathcal{L}_I = \int_{-\infty}^{-R} d\rho \int_0^R d\lambda \; \frac{\rho\,\lambda^2}{-\sqrt{\lambda^2 + r^2}} \; e^{-iE\sqrt{\lambda^2 + r^2}} \; f(\rho) \tag{22}$$

which can now be combined with S_I to give

$$S_I + \mathcal{L}_I = \int_{-\infty}^{-R} d\rho \; \rho \; f(\rho) \int_0^{\infty} d\lambda \; \frac{\lambda^2}{-\sqrt{\lambda^2 + r^2}} \; e^{-iE\sqrt{\lambda^2 + r^2}} \; . \tag{23}$$

The change of variable

$$u = \sqrt{\left(\frac{\lambda}{r}\right)^2 + 1} \; . \tag{24}$$

Then yields.

$$S_I + \mathcal{L}_I = -\int_{-\infty}^{-R} d\rho \; f(\rho) \; \rho^3 \int_1^{\infty} du \; \sqrt{u^2 - 1} \; e^{-iE\,r\,u} \; . \tag{25}$$

We must now face the problem, which we ignored above, that the u integration is divergent. However it is a limiting case of a convergent integral, namely when r has a negative imaginary part. This means we are dealing with generalized functions and we shall define this integral and others to follow as the limit as parameters approach their value through values which make the integral convergent. These statements although applied here to the u integration actually refer to the method of interpretation of the original α integrations. With this

interpretation we now have[14]

$$S_I + \mathcal{L}_I = -\int_{-\infty}^{-R} d\rho\, f(\rho)\, \rho^3 \left\{ \frac{i\pi}{2Er} H_1^{(2)}(Er) \right\} . \tag{26}$$

An exactly analogous calculation, this time using

$$\rho = \sqrt{\alpha^2 - \lambda^2} = r \; ; \; r > 0 \tag{27}$$

$$\alpha = \sqrt{\rho^2 + \lambda^2} = \sqrt{\lambda^2 + r^2}$$

yields

$$S_{IV} + \mathcal{L}_{II} = \int_R^{\infty} d\rho\, f(\rho)\, \rho^3 \left\{ \frac{-i\pi}{2Er} H_1^{(1)}(Er) \right\} . \tag{28}$$

We shall now consider S_{II} :

$$S_{II} = \int_R^{\infty} d\lambda \int_{-\sqrt{\lambda^2 - R^2}}^{0} d\alpha\, \lambda^2\, e^{i\alpha E}\, f\left(\sqrt{\alpha^2 - \lambda^2}\right) . \tag{29}$$

Upon using the change of variables defined by

$$\begin{aligned} \rho &= \sqrt{\alpha^2 - \lambda^2} = -ir \; ; \; r > 0 \\ \alpha &= \sqrt{\rho^2 + \lambda^2} = -\sqrt{\lambda^2 - r^2} \end{aligned} \tag{30}$$

we obtain

$$S_{II} = \int_R^{\infty} d\lambda \int_{-iR}^{-i\lambda} d\rho \; \rho \; f(\rho) \; \frac{\lambda^2}{-\sqrt{\lambda^2 - r^2}} \; e^{-i E \sqrt{\lambda^2 - r^2}} \tag{31}$$

$$= \int_{-iR}^{-i\infty} d\rho \; f(\rho) \; \rho \int_r^{\infty} d\lambda \; \frac{\lambda^2}{-\sqrt{\lambda^2 - r^2}} \; e^{-i E \sqrt{\lambda^2 - r^2}} \; .$$

The further change of variable

$$u = \sqrt{\left(\frac{\lambda}{r}\right)^2 - 1} \tag{32}$$

gives

$$S_{II} = \int_{-iR}^{-i\infty} d\rho \; f(\rho) \; \rho^3 \int_0^{\infty} du \; \sqrt{u^2 + 1} \; e^{-iEru} \; . \tag{33}$$

The analogous calculation for S_{III} is made by setting

$$\begin{aligned} \rho &= \sqrt{\alpha^2 - \lambda^2} = -i\, r \; ; \quad r > 0 \\ \alpha &= \sqrt{\rho^2 + \lambda^2} = \sqrt{\lambda^2 - r^2} \end{aligned} \tag{34}$$

and yields

$$S_{III} = -\int_{-i\infty}^{-iR} d\rho \; f(\rho) \; \rho^3 \int_0^{\infty} du \; \sqrt{u^2 + 1} \; e^{iEru} \tag{35}$$

Now, in a manner consistent with our interpretation of the u integrals, we can deform the u contours through the convergent quadrant to the imaginary axis, avoiding the branch points at $\pm i$ in the appropriate manner. Then introducing the variable $v = i\,u$ the u integration in S_{II} becomes

$$-\int_1^\infty dv\,\sqrt{v^2-1}\;e^{-Erv} - i\int_0^1 dv\,\sqrt{1-v^2}\;e^{-Erv}\,. \qquad (36)$$

Upon setting $v = -i\,u$, the u integration in S_{III} gives

$$-\int_1^\infty dv\,\sqrt{v^2-1}\;e^{-Erv} + i\int_0^1 dv\,\sqrt{1-v^2}\;e^{-Erv}\,. \qquad (37)$$

The integral between finite limits will cancel in the sum of S_{II} and S_{III}, and thus we may take[15]

$$S_{II} = S_{III} = -\int_{-iR}^{-i\infty} d\rho\, f(\rho)\,\rho^3 \int_1^\infty dv\,\sqrt{v^2-1}\;e^{-Erv} \qquad (38)$$

$$= \int_{-iR}^{-i\infty} d\rho\, f(\rho)\,\rho^3 \left\{ -\frac{K_1(Er)}{Er} \right\}\,.$$

The results at this point may be summarized by[16]

$$S_I + \mathcal{L}_I = \int_{-\infty}^{-R} d\rho\, f(\rho)\, \rho^2 \left\{ \frac{i\pi}{2E}\, H_1^{(2)}(E\rho\, e^{i\pi}) \right\}$$

$$S_{II} = S_{III} = \int_{-iR}^{-i\infty} d\rho\, f(\rho)\, \rho^2 \left\{ \frac{-i\pi}{2E}\, H_1^{(2)}(E\rho) \right\} \tag{39}$$

$$\mathcal{L}_{II} + S_{IV} = \int_{R}^{\infty} d\rho\, f(\rho)\, \rho^2 \left\{ \frac{-i\pi}{2E}\, H_1^{(1)}(E\rho) \right\} .$$

To evaluate the loop integrals (Figures 1 and 2) we let

$$\alpha = \sqrt{\lambda^2 + R^2\, e^{2i\theta}} \tag{40}$$

in both L_I and $\mathcal{L}_I$, then take θ as the new variable. For both L_I and $\mathcal{L}_I$ the range of θ is

$$-\pi < \theta < -\frac{\pi}{2} . \tag{41}$$

We now add $\mathcal{L}_I$ and L_I. This leads to the result that λ ranges from zero to infinity, and if we let $\rho = R\, e^{i\theta}$ we have

$$L_I + \mathcal{L}_I = \int_{-R}^{-iR} d\rho\, \rho\, f(\rho) \int_0^{\infty} d\lambda\, \frac{\lambda^2}{\sqrt{\lambda^2 + \rho^2}}\, e^{iE\sqrt{\lambda^2 + \rho^2}} . \tag{42}$$

The phase of the square root is such that it becomes a negative real quantity as ρ becomes real and negative. Thus the function represented by the λ integration is the analytic continuation of the corresponding function in $S_I + \mathcal{L}_I$ as ρ follows the circular arc from $-R$ to $-iR$.

The corresponding calculation for $\mathcal{L}_{II} + L_{II}$ yields the corresponding continuation of $S_{IV} + \mathcal{L}_{II}$, with the net result that the R limits on the remaining ρ integration in $S_I + \mathcal{L}_I$ and $S_{IV} + \mathcal{L}_{II}$ can be replaced by $-iR$ upon adding the contribution of the loop integrals.

Consider the integrals for S_{II} or S_{III}. These contours may be deformed, by Jordan's lemma, to go to infinity along the real axis, and therefore may be combined with the other integrals. This gives

$$S_{II} + S_I + L_I + \mathcal{L}_I + \mathcal{L}_I = \int_{-\infty}^{-iR} d\rho \quad \rho^2 f(\rho) \left\{ \frac{i\pi}{2E} \left[H_1^{(2)}(E\rho\, e^{i\pi}) + H_1^{(2)}(E\rho) \right] \right\}$$

$$S_{III} + S_{IV} + L_{II} + \mathcal{L}_{II} + \mathcal{L}_{II} = \int_{-iR}^{\infty} d\rho\, \rho^2 f(\rho) \left\{ \frac{-i\pi}{2E} \left[H_1^{(1)}(E\rho) + H_1^{(2)}(E\rho) \right] \right\} . \tag{43}$$

Now the sum of the Hankel functions yields $-2J_1(E\rho)$ in the first case[17] and $2J_1(E\rho)$ in the second, so the two pieces may be added to yield a single contour integral. This gives

$$S_n\,(E, m_i) = \frac{-i}{(2\pi)^2 E} \int d\rho\, \rho^2 f(\rho)\, J_1(E\rho) \tag{44}$$

where

$$f(\rho) = \prod_{k=1}^{n} \left[\frac{2\pi^2 i\, m_k}{\rho} \quad H_1^{(2)}\,(m_k\, \rho) \right] . \tag{45}$$

The ρ contour runs from minus infinity to infinity below the origin. If this contour is chosen to be symmetric under $\rho \to e^{-i\pi}\rho^*$ then it can be shown that the contribution from the left half of the contour is the negative complex conjugate of the contribution from the right half. Thus, because of the factor i multiplying the integral, the above expression for S_n is real, as is required.

We note that if we write $J_1 = \frac{1}{2}\left(H_1^{(1)} + H_1^{(2)}\right)$ in Eq. (44) then the integral involving $H_1^{(2)}$ vanishes and we may write

$$S_n(E,m_i) = \frac{-i}{2(2\pi)^2 E} \int d\rho\, \rho^2\, f(\rho)\, H_1^{(1)}(E\rho) \quad . \tag{46}$$

This form will be convenient for consideration of the non-relativistic limit.

IV. EVALUATION OF THE INTEGRAL

The integrand of the expression for S_n (Eq. 44) is, apart from constant, real factors

$$g(\rho) = -i\rho^2 J_1(E\rho) \prod_{k=1}^{n} \left[\frac{H_1^{(2)}(m_k\rho)}{-i\rho} \right] . \tag{47}$$

This function has a single saddle point on the negative imaginary axis because there it takes the form[16]

$$g(-iy) = y^2 I_1(Ey) \prod_{k=1}^{n} \left[\frac{2}{\pi} \frac{K_1(m_k y)}{y} \right] . \tag{48}$$

The function $g(\rho)$ also has many saddle points in the neighborhood of the real axis.[18] These define paths of constant phase between the zeroes of J_1. Since $g(\rho)$ alternates in sign in different sections, large cancellations are expected to occur. We thus expect that the dominant contribution to the integral, taken along a path of constant phase, comes from the neighborhood of the saddle point on the negative imaginary axis. If we denote this point by ρ_o then the standard saddle point approximation yields

$$S_n \sim g(\rho_o) \left[\frac{2\pi}{-\frac{d^2}{d\rho^2} \log g(\rho_o)} \right]^{\frac{1}{2}} . \tag{49}$$

This approximation then allows us to compute S_n. In the following we shall investigate the accuracy of this approximation in the non-

relativistic and "ultra-relativistic" limits.

To examine the non-relativistic limit let us turn to the second form for S_n, Eq. 46, and insert asymptotic expansions for the Hankel functions.[19] After some rearrangement this yields

$$S_n \sim (2\pi)^{\frac{3}{2}(n-1)} \frac{1}{\Pi^{\frac{1}{2}}} E^{-\frac{3}{2}} \sum_{\ell=0}^{\infty} \frac{(-1)^{\ell}(1,\ell)}{(2E)^{\ell}} \sum_{j_1=0}^{\infty} \cdots \sum_{j_n=0}^{\infty}$$

$$\left[\prod_{k=1}^{n} \frac{(1,j_k)}{(2m_k)^{j_k}}\right] \left\{ \frac{i^{\frac{5}{2}(n-1)-\ell-\Sigma j_k}}{2\pi} \int d\rho \; e^{iT\rho} \; \rho^{-\frac{3}{2}(n-1)-\ell-\Sigma j_k} \right\} . \tag{50}$$

We have used the abbreviation Π for the product of the masses and will use Σ for their sum. If the contour is now deformed to go to $i\infty$ at both ends and the change of variable $t = -i\rho T$ is made the term in braces becomes[20]

$$\frac{T^{\frac{3}{2}n - \frac{5}{2} + \ell + \Sigma j_k}}{\Gamma(\frac{3}{2}n - \frac{3}{2} + \ell + \sum_k j_k)} . \tag{51}$$

Now if the inverse powers of E are expanded and terms are collected we have obtained an asymptotic expansion of S_n in powers of T. The first term of this expansion is

$$S_n^{N.R.} = (2\pi)^{\frac{3}{2}(n-1)} \frac{1}{\Pi^{\frac{1}{2}}} \Sigma^{-\frac{3}{2}} \frac{T^{\frac{3}{2}n - \frac{5}{2}}}{\Gamma(\frac{3}{2}n - \frac{3}{2})} . \tag{52}$$

This agrees with the phase space computed by more elementary methods (See Appendix III).

In this limit we can examine the saddle point approximation. The saddle point is located at

$$\rho_o = -i \frac{\frac{3}{2}n - \frac{3}{2}}{T} . \tag{53}$$

Application of the saddle point method to the integral yields the above result with the Γ function replaced by the first term of Stirling's approximation to it. For $n = 2$ this approximation is already very good (about 6% accuracy), for $n = 3$ it is accurate to better than 3% and it improves with increasing n. We note that this estimate applies only when $E\rho_o$ is large, that is

$$(\frac{3}{2}n - \frac{3}{2}) \frac{m_k}{T} \gg 1 \tag{54}$$

otherwise the saddle point of the original integral would not occur in the asymptotic region of the Hankel functions.

The other case for which we can estimate the accuracy of the saddle point method is that one in which it is a good approximation to replace $H_1^{(1)}(E\rho)$ by its asymptotic value and $H_1^{(2)}(m_k\rho)$ by its value for small argument. This will be seen to be very close to the ultra-relativistic limit. If this is done we find

$$f(\rho) = \left(\frac{-4\pi}{\rho^2} \right)^n \quad . \tag{55}$$

Steps similar to those used in the non-relativistic case lead to

$$S_n^{\text{U.R.}} = \frac{(4\pi)^n}{(2\pi)^{\frac{3}{2}}} \frac{E^{2n-4}}{\Gamma(2n - \frac{3}{2})} \tag{56}$$

and again the saddle point method is equivalent to replacing the Γ function by the first term of Stirling's approximation. For $n = 2$ this approximation is accurate to 3% and improves with increasing n. The saddle point now occurs at

$$\rho = -i \frac{2n - \frac{3}{2}}{E} \tag{57}$$

and thus this estimate applies if

$$\begin{aligned} 2n - \frac{3}{2} &\gg 1 \\ (2n - \frac{3}{2}) \frac{m_k}{E} &\ll 1 \quad . \end{aligned} \tag{58}$$

The true ultra-relativistic limit may be obtained by identifying it with the limit of zero mass, thus

$$S_n(E,0) = \frac{-i}{(2\pi)^2 E} \int d\rho \, \rho^2 J_1(E\rho) \left(\frac{-4\pi}{\rho^2} \right)^n \quad . \tag{59}$$

This integration may be performed by taking the contour to be the real axis excluding -1 to 1 and the lower half of the unit circle. The integrals along the real axis cancel since J_1 is an odd function, while the integral along the unit circle may be easily performed if we insert the power series expansion for J_1 [21]. The result is

$$S_n(E,0) = \frac{2\,\Pi^{n-1}}{(n-1)!\,(n-2)!}\,E^{2n-4} \quad . \tag{60}$$

The ratio of this to $S_n^{U.R.}$ approaches 1 with reasonable rapidity as n increases. This is to be expected, for as n increases the saddle point of this integral moves into the asymptotic region of J_1 where the saddle point method was applied to find $S_n^{U.R.}$.

V. ISOTOPIC SPIN COEFFICIENTS

In order to complete the calculation based on the phase space model, we must now determine the isotopic spin coefficients, $\left(\Gamma_{t_i\theta_i}{}^{T}\right)^2$. If we consider a state defined by the isotopic spin of its constituents, t_i, and their third components, θ_i, then these coefficients are defined in terms of a projection operator, P_T, onto states of well defined total isotopic spin, T, by

$$(\Gamma_{t_i\theta_i}{}^{T})^2 = |P_T\,|t_1\theta_1,\cdots,t_n\theta_n\rangle|^2 = \langle t_i\theta_i|\,P_T\,|t_i\theta_i\rangle \quad . \tag{61}$$

We now use a standard form for the projection operator[22] in terms of the Hurwitz integral over the rotation group, which in an Euler angle parameterization is

$$P_T = \frac{2T+1}{8\pi^2}\int_0^{2\pi} d\alpha\, d\gamma \int_0^{\pi} d\,\beta\, \sin\beta\, \chi^{(T)*}(\alpha,\beta,\gamma)\, R(\alpha,\beta,\gamma) \quad . \tag{62}$$

In this expression $\chi^{(T)}(\alpha,\beta,\gamma)$ is the character of the rotation defined by (α,β,γ) in the representation of dimension $2T+1$, and $R(\alpha,\beta,\gamma)$ is a rotation operator for those angles. The required matrix element of this rotation operator is then simply

$$\prod_{i=1}^{n} D_{\theta_i\theta_i}^{(t_i)}(\alpha,\beta,\gamma) \tag{63}$$

where the D functions are the usual representations of the rotation

group. Now we note that by definition

$$\chi^{(T)}(\alpha,\beta,\gamma) = \sum_{m=-T}^{T} D_{mm}^{(T)}(\alpha,\beta,\gamma) \quad . \tag{64}$$

We also have[23]

$$D_{mm}^{(T)}(\alpha,\beta,\gamma) = \sum_{\nu} (-1)^{\nu} \binom{T+m}{\nu}\binom{T-m}{\nu}\left(\frac{1-\cos\beta}{1+\cos\beta}\right)^{\nu} \left(\frac{1+\cos\beta}{2}\right)^{T} e^{im(\alpha+\gamma)} \tag{65}$$

$$= e^{im(\alpha+\gamma)} \; d_{mm}^{T}(\cos\beta) \quad .$$

Upon combining these expressions and substituting the resulting character into the integral we find that

$$(\Gamma_{t_i\theta_i}^{T})^2 = \frac{2T+1}{8\pi^2}\int_0^{2\pi} d\alpha\, d\gamma \int_{-1}^{1} d\mu \left[\sum_{m=-T}^{T} d_{mm}^{T}(\mu)\, e^{i(M-\mu)(\alpha+\gamma)}\right] \tag{66}$$

$$\prod_{i=1}^{n} d_{\theta_i\theta_i}^{t_i}(\mu)$$

where $M = \sum_{i=1}^{n} \theta_i$ and $\mu = \cos\beta$. But since

$$\int_0^{2\pi} d\alpha\, d\gamma \; e^{i(M-m)(\alpha+\gamma)} = (2\pi)^2 \; \delta_{M,m} \tag{67}$$

(which simply expresses conservation of T_3) we have

$$(\Gamma_{t_i\theta_i}{}^T)^2 = \frac{2T+1}{2}\int_{-1}^{1} d\mu\, D_{MM}{}^T(\mu) \prod_{i=1}^{u} d_{\theta_i\theta_i}{}^{t_i}(\mu) \quad . \tag{68}$$

An important simplification can be made if we restrict ourselves to isotopic spins $\frac{3}{2}$ or less. The following properties then facilitate the computation of all the relevant d^T functions

$$\begin{aligned} d_{mm}{}^T(\mu) &= d_{-m,-m}{}^T(\mu) \quad ; \quad d_{TT}{}^T(\mu) = \left(\frac{1+\mu}{2}\right)^T \\ d_{00}{}^1(\mu) &= \mu \quad ; \quad d_{00}{}^0(\mu) = 1 \quad ; \quad d_{\frac{1}{2}\frac{1}{2}}{}^{\frac{3}{2}}(\mu) = \frac{3\mu-1}{2} \quad . \end{aligned} \tag{69}$$

We now introduce the following counting scheme. Let $n_t{}^\theta$ be the number of particles of isospin t and third component θ, and include the initial state in this number. Then we define

$$\begin{aligned} i &= \sum_{t=0}^{\frac{3}{2}} \sum_{\theta=-t}^{t} |\theta|\, n_t{}^\theta \\ j &= n_1{}^0 \\ k &= n_{\frac{3}{2}}{}^{\frac{1}{2}} + n_{\frac{3}{2}}{}^{-\frac{1}{2}} \quad . \end{aligned} \tag{70}$$

Now the integral can be written as

$$(\Gamma_{t_i \theta_i}{}^T)^2 = \frac{2T+1}{2^{i+k+1}} \int_{-1}^{1} d\mu \, (1+\mu)^i \, \mu^j \, (3\mu-1)^k = P_{i,j,k}{}^T \qquad (71)$$

We note that, for any state which conserves total isotopic spin, i is an integer. Using this form we can easily obtain the following recursion relations.

$$P_{ojo}{}^T = \frac{2T+1}{j+1} \, \delta_{j,2n} \quad n \text{ any integer}$$

$$P_{i+1,j,k}{}^T = \frac{1}{2} \left(P_{ijk}{}^T + P_{i,j+1,k}{}^T\right) \qquad (72)$$

$$P_{i,j,k+1}{}^T = \frac{1}{2} \left(3 \, P_{i,j+1,k}{}^T - P_{ijk}{}^T\right)$$

Thus the isotopic spin coefficients are easily calculated with a high-speed computer (or even pencil and paper).

VI. CALCULATION OF SPECTRA

We can also reasonably expect the phase space model to predict energy distributions of final state particles averaged over all angles of emission. To obtain this prediction we simply do not integrate over the momenta of the particle in question. Let this particle be labeled particle 1, then

$$S_n(P,m_i) = \int \frac{d^3p_1}{\omega_1} \int \delta^{(4)}\left(P-p_1-\sum_{i=2}^{n} p_n\right) \prod_{i=2}^{n} \frac{d^3p_i}{\omega_i}$$
$$= \int \frac{d^3p_1}{\omega_1} S_{n-1}(P-p_1, m_i) \quad . \tag{73}$$

We now use the Lorentz invariance of S_{n-1} to evaluate it in the center of mass system for $P - p_1$. It is then clearly independent of the direction of $\vec{p}_1$, so

$$S_n(E,m_i) = 4\pi \int p_1 \, d\omega_1 \, S_{n-1}\left(E' = \sqrt{E^2 - 2E\omega_1 + m_1^2}\,,\ m_i\right). \tag{74}$$

Thus if we denote the unnormalized probability of obtaining the final state f containing the particle 1 with energy ω and having a total energy E by $P_f(E,\omega)$ we have

$$P_f(E,\omega) = \frac{\prod_{i=1}^{n} v_i(2s_i+1)}{\prod_j n_j\,!} \left(\Gamma_{t_i\theta_i}T\right)^2 4\pi \sqrt{\omega^2 - m_1^2}$$
$$S_{n-1}\left(\sqrt{E^2 - 2E\,\omega + m_1^2}\,,\ m_i\right). \tag{75}$$

This calculation is straight forward, however due to our inclusion of resonances as final state particles it yields the spectrum of these resonances, not the observed final state particles. To obtain the observed spectra we must determine the spectra of decay products of resonances, given the spectra of the resonances and their decay modes.[24]

Let us denote quantities refering to the resonance by capital letters, and to a decay product by small letters. Let starred quantities refer to the C.M. frame of the resonance, Σ^*, and un-starred quantities to any other frame Σ (which will later be taken to be the C.M. frame of the entire reaction). Then the momentum and energy of the resonant state in Σ determine the Lorentz transformation parameters between Σ and Σ^*. Thus we have

$$e = \gamma(e^* + \beta\, p^* \cos\theta^*) \tag{76}$$

where

$$\beta = \frac{P}{E} \qquad \gamma = \frac{E}{M} \tag{77}$$

and θ is the angle between $\vec{p}^*$ and $\vec{p}$. Now let n be the number of decays, then

$$\frac{dn}{de} = \frac{dn}{d(\cos\theta^*)} \frac{d(\cos\theta^*)}{de} = \frac{dn}{d(\cos\theta^*)} \frac{1}{\beta p^*} \quad . \tag{78}$$

If the decay spectrum is independent of $\cos\theta$ (which is certainly true if the resonances are not polarized) as we shall assume, then the spectrum of particles of a given energy in Σ^* will be constant in Σ. If e_+ and e_- are the maximum and minimum possible energies in Σ, the normalized spectrum is simply $(e_+ - e_-)^{-1}$. Explicitly we have

$$e_\pm = \frac{E\,e^*}{M} \pm \frac{P\,p^*}{M} \quad . \tag{79}$$

If we now have a spectrum, $W(E)$, of resonances and a decay spectra, $w^*(e^*)$, we can obtain the decay spectra in Σ by

$$w(e) = \int_0^\infty dE \int_0^\infty de^* \; \frac{W(E)\; w^*(e^*)}{e_+ - e_-} \; S\,(e,E,e^*) \tag{80}$$

where

$$S(e,E,e^*) = \theta(e-e_-) - \theta(e-e_+) \tag{81}$$

defines the actual domain of integration in terms of the usual step functions θ. This can be written as

$$w(e) = \frac{M}{2} \int de^* \; \frac{w^*(e^*)}{p^*} \int_{E_-}^{E_+} dE \; \frac{W(E)}{P} \tag{82}$$

where

$$E_{\pm} = \frac{M}{m} \quad \frac{e\, e^{*} \pm p\, p^{*}}{m} \quad . \tag{83}$$

The e^{*} integration runs over the allowed decay energies. For this calculation we are interested only in two and three body decay modes. The two body spectra $w^{*}(e^{*})$ is simply a δ-function. For the three body modes we shall assume $w^{*}(e^{*})$ is given by phase space (since this is itself a spectrum the three body modes require only knowledge of the two body phase space).

VII. RESULTS

Since the results of this investigation are predominately negative with respect to its primary aims, I shall not give a detailed description of the various calculations but merely try to indicate typical results and their inadequacies.

Due to the rapid rate of discovery of new resonances, this calculation must be incomplete. A list of the particle states included will be found in Table I, however most of the calculations have neglected the stronge particles, which is an adequate approximation within the expected accuracy of the model.

A. $\bar{p}$ - p Interactions

One of the early problems attacked with the Fermi model was the pion multiplicity in antiproton annihilations at rest.[25] It was found that the interaction volumes had to be increased about tenfold to agree with experimental results.

The inclusion of resonances in the present calculation has achieved good agreement with measured multiplicities without modification of the volume factors (that is all $\xi_i = 1$). These results are presented in Table II. The calculated spectrum of charged pions (Fig. 3) is however in poor agreement with experimental data.[26] It was found that a ξ factor of 0.1 for the rho meson would improve the spectra without disturbing the multiplicities excessively (see Fig. 3 and Table III). However, this limited agreement seems to be fortuitous in the light of more recent experiments[25] which demonstrate that multiple resonance

TABLE I

"Particles" included in the calculation.

Non-Strange	Strange
π	K
nucleon	Λ
deuteron	Σ
ρ	Ξ
$N^*(1238)$	$Y_1^*(1385)$
ω	$Y_0^*(1405)$
η	$Y_0^*(1520)$
$N^*(1512)$	$Y_0^*(1815)$
$N^*(1688)$	$K^*(885)$
$N^*(1920)$	$K^*(730)$
	$Y_1^*(1660)$

TABLE II

Pion and charged prong multiplicities in $\bar{p}$-p annihilations at rest with $v_\rho = 1$ and assuming pure T = 1.

n_{ch}	% Theo.	% Exp.
0	1.9	3.0
2	45.0	42.0
4	53.0	51.0
6	1.0	4.0
avg.	3.03	3.12 ± 0.11

n_π	% Theo.	% Exp.
0	0.93	
1	0.46	
2	3.71	
3	5.10	
4	27.48	
5	47.68	
6	8.78	
7	5.72	
8	0.14	
avg.	4.65	4.78 ± 0.17

$n_{\pi^\pm}$	% Theo
0	2.40
2	44.48
4	53.01
6	0.10
avg.	3.02

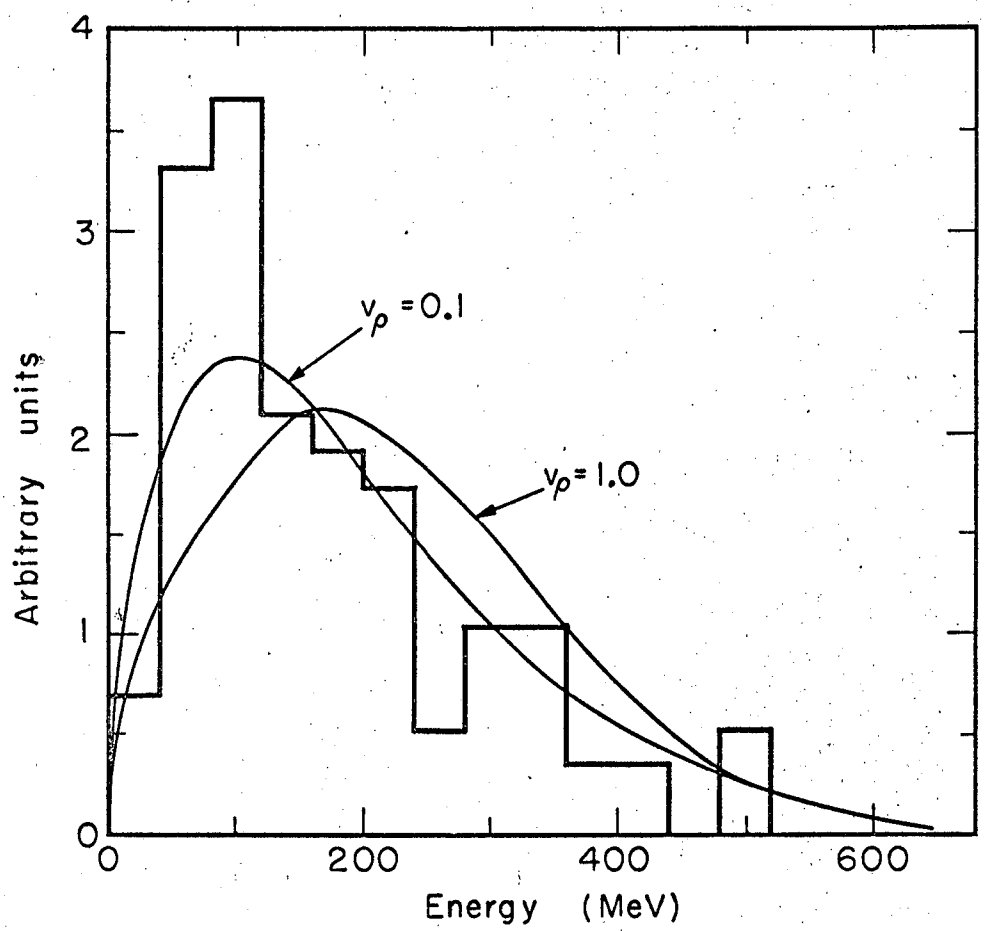

MU-36511

Fig. 3. Pion spectra from $\bar{p}$ - p annihilation at rest. Smooth curves are theoretical predictions normalized to the total number of experimental tracks.

TABLE III

Pion and charged prong multiplicities in $\bar{p}$-p annihilations at rest with $v_\rho = 0.1$ and assuming equal $T = 0$ and $T = 1$ contributions.

n_{ch}	% Theo.	$n_{\pi^\pm}$	% Theo.
0	6.5	0	8.2
2	39.9	2	38.2
4	53.4	4	53.4
6	0.2	6	0.2
avg.	2.95	avg.	2.91

Average number of pions 5.01

production is quite rare (e.g. a branching ratio of 0.006 ± 0.003 for the $\omega\rho$ final state) while these states dominate the calculation (e.g. a calculated branching ratio of 0.30 for the $\omega\rho$ final state assuming pure I-spin 1). Table IV lists the dominant contributions to the calculation.

A cursory examination of the frequency of $K\bar{K}$ pairs indicates that the volume factors of the K-π resonances should be increased by a factor of 6 or 7 to achieve agreement with experiments.[27]

B. p - p Interactions

In our analysis of the p - p interaction we attempted to fit the energy dependence of gross features of the reaction and the shape of the spectra of emitted particles.

1. Gross Features

Our primary concern was to fit the variation of the average number of charged particles emitted, denoted $\langle n_{ch} \rangle$, and the relative probability of a given number, denoted n_{ch}. The "straight-forward" prediction of the model (all $\xi_i = 1.0$) overestimates $\langle n_{ch} \rangle$ badly (Fig. 4) and the disagreement increases with the energy.[29] If we attempt to improve this situation by decreasing all the ξ_i uniformly, the high energy behavior can be improved but the overall fit is not. If the ξ_i corresponding only to the resonant states, denoted ξ_i^*, are reduced to 0.05 we obtain the second curve in Fig. 4. The justification for this procedure is basically empirical, however this step was initially taken to crudely account for the very short

TABLE IV

T = 1		T = 0	
State	Branching Ratio	State	Branching Ratio
$\rho^-\pi^+$	0.013	$\pi^+\pi^-\pi^0$	0.002
$\rho^-\pi^0\pi^+$	0.018	$\rho^-\pi^+$	0.013
$\rho^0\pi^0\pi^0$	0.013	$\rho^-\pi^0\pi^+$	0.012
$\rho^0\pi^+\pi^-$	0.018	$\rho^-\pi^0\pi^0\pi^+$	0.002
$\rho^+\pi^-$	0.013	$\rho^-\pi^+\pi^+\pi^-$	0.002
$\rho^+\pi^-\pi^0$	0.018	$\rho^0\pi^0$	0.013
$\rho^-\rho^0\pi^+$	0.021	$\rho^0\pi^-\pi^+$	0.012
$\rho^0\rho^0\pi^0$	0.016	$\rho^0\pi^+\pi^-\pi^0$	0.003
$\rho^-\rho^+$	0.149	$\rho^+\pi^-$	0.013
$\rho^-\rho^+\pi^0$	0.021	$\rho^+\pi^-\pi^0$	0.012
$\rho^0\rho^+\pi^-$	0.021	$\rho^+\pi^-\pi^0\pi^0$	0.002
$\omega\pi^0$	0.026	$\rho^+\pi^-\pi^-\pi^+$	0.002
$\omega\pi^+\pi^-$	0.021	$\rho^-\rho^0\pi^+$	0.014
$\omega\rho^-\pi^+$	0.021	$\rho^0\rho^0$	0.079
$\omega\rho^0$	0.298	$\rho^-\rho^+$	0.157
$\omega\rho^+\pi^-$	0.021	$\rho^-\rho^+\pi^0$	0.014
$\omega\omega\pi^0$	0.017	$\rho^0\rho^+\pi^-$	0.014
$\eta\pi^+\pi^-$	0.009	$\omega\pi^0\pi^0$	0.011
$\eta\pi^0$	0.007	$\omega\pi^-\pi^+$	0.022
$\eta\rho^-\pi^+$	0.026	$\omega\pi^-\pi^0\pi^+$	0.004
$\eta\rho^0$	0.088	$\omega\rho^-\pi^+$	0.023
$\eta\rho^+\pi^-$	0.026	$\omega\rho^0\pi^0$	0.023
$\omega\eta\pi^0$	0.049	$\omega\rho^+\pi^-$	0.023
$\eta\eta\pi^0$	0.015	$\omega\omega$	0.235

TABLE IV (Cont.)

T = 0	
State	Branching Ratio
$\eta\pi^0\pi^0$	0.004
$\eta\pi^+\pi^-$	0.009
$\eta\pi^+\pi^-\pi^0$	0.003
$\eta\rho^-\pi^+$	0.028
$\eta\rho^0\pi^0$	0.028
$\eta\rho^+\pi^-$	0.028
$\omega\eta$	0.140
$\eta\eta$	0.019
$\eta\eta\eta$	0.005

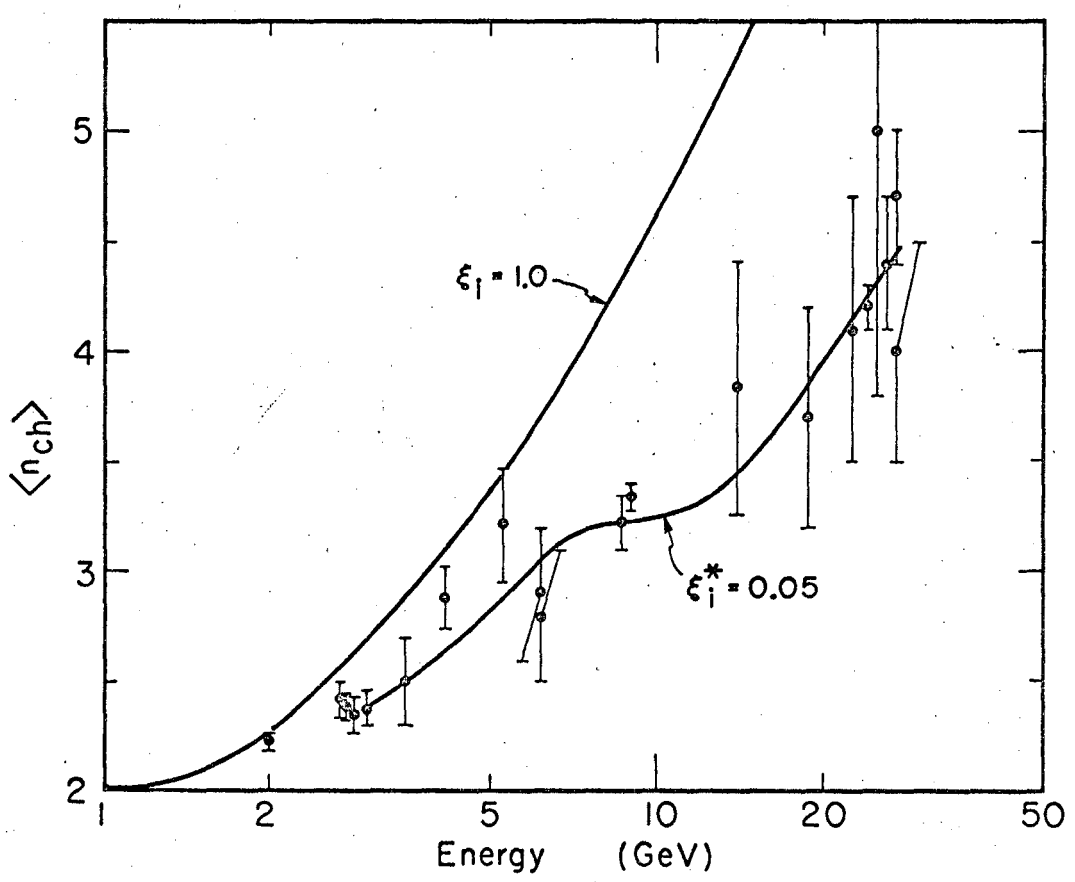

MU-36512

Fig. 4. The variation of $\langle n_{ch} \rangle$ with energy for p - p collisions.

lifetime of these particles and the corresponding likelihood they would not escape from the "hot spot." In view of the nature of the data and the expected accuracy of the model one might be tempted to claim this is a reasonable fit. However any attempt to extrapolate using this model is likely to be very incorrect, since apparently above 15 GeV the curve is resuming the very rapid increase that was the failure of the "straight forward" calculation. The cause of the leveling of this curve in the region 7 to 13 GeV is unclear since the computer is considering a large number of final states (<1000) and $\langle n_{ch} \rangle$ depends on a rather delicate and intricate relationship among them.

The problem with the high energy behavior may be made clearer by consideration of some numbers. If we fit the form

$$n(E) = a E^{x} \tag{84}$$

to $\langle n_{ch} \rangle$, then a very rough fit to the upper end of these curves yields $x = .62$ for the $\xi_i = 1$ case and $x = .46$ for the $\xi_i^* = .05$ case. In the high energy limit for the phase space model we have[28] $x = 2/3$ (this limit is approached very slowly) and yet cosmic ray data indicates we need $x \simeq 1/4$, although accelerator data only may be fit with $x \simeq 1/2$.[29]

The percentages of final states with n charged prongs in the final state are plotted in Figures 5 and 6. The theoretical curves are for $\xi_i^* = .05$.[30] This data forms a more sensitive test but by its nature is subject to much larger experimental errors. These curves

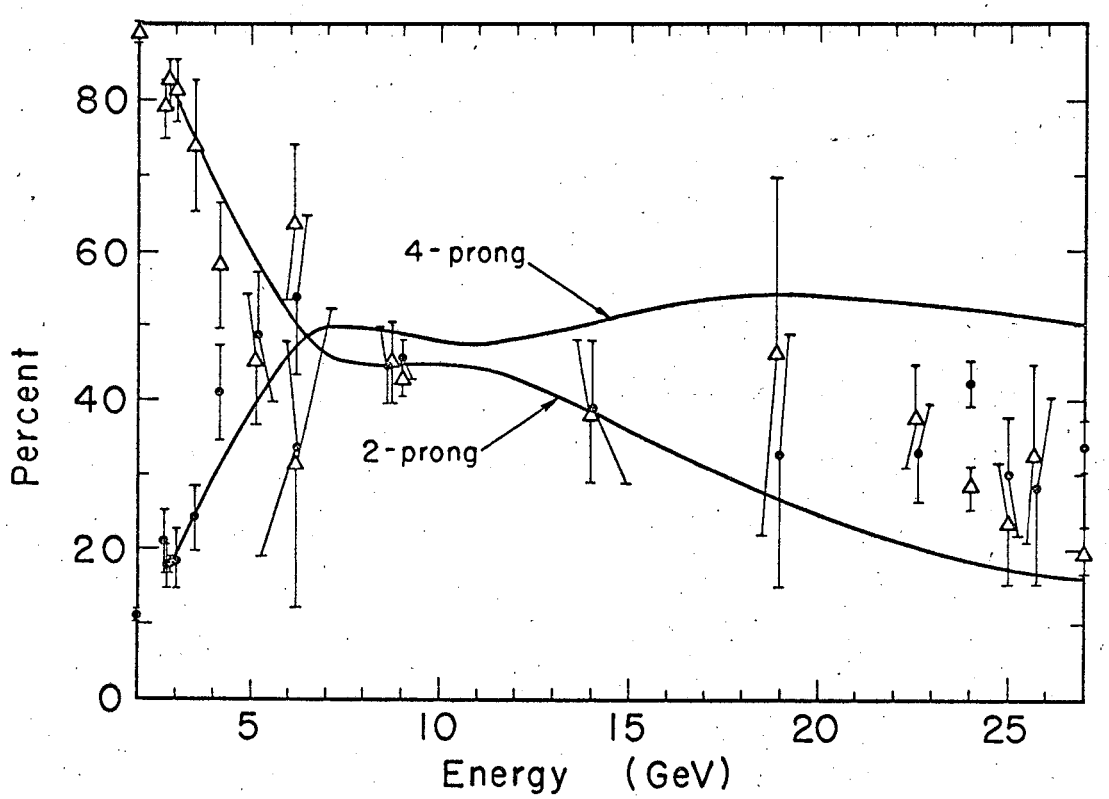

MU-36513

Fig. 5. The variation of the percentage of two and four prong final states with energy in p - p collisions. Triangles are two prong data points and circles are four prong data.

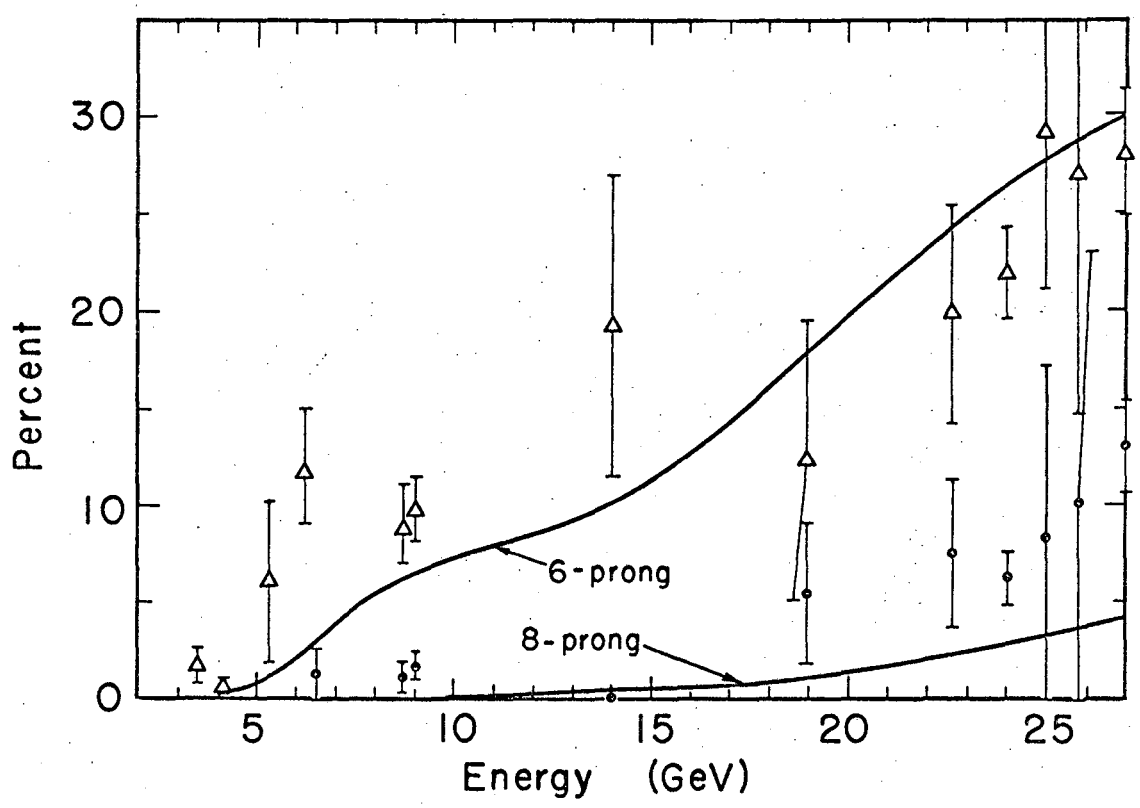

MU-36514

Fig. 6. The variation of the percentage of six and eight prong final states with energy in p - p collisions. The triangles are six prong data and the circles are eight prong data.

demonstrate that the nature of the failure to adequately fit the $\langle n_{ch} \rangle$ data is an overemphasis of states near the mean rather than inclusion of too many states of very high multiplicity. A narrow dispersion about $\langle n_{ch} \rangle$ is expected (at least asymptotically) from a statistical model without resonances.[31]

2. Spectra

The pion and proton spectra were studied from primary proton beam energies of 2.75, 4.2, 6.2, 9, 12, 19.8 GeV. We will discuss the results at 6.2 GeV only since similar problems in fitting the data for all energies were encountered.

Both the experimental[32] and theoretical[33] pion spectra are presented in Fig. 7 as histograms with the same normalization. As can readily be seen, the peak of the theoretical spectrum is about 200 MeV/C higher than that of the experimental spectrum. Apparently, the location of this maximum is an approximate invariant of the phase space model. It, like the experimental data, shifts only slightly with changes in the incident energy. The location of the peak is also very insensitive to changes in the ξ_i factors, although the shape of the entire curve can be radically changed by modification of the ξ_i. Hence the model predicts far too many high energy pions, and drastic changes of the ξ_i would be required to alter this situation. We believe that the limited agreement with the crude features of the interaction (multiplicities, etc.) could not be maintained were such changes made.

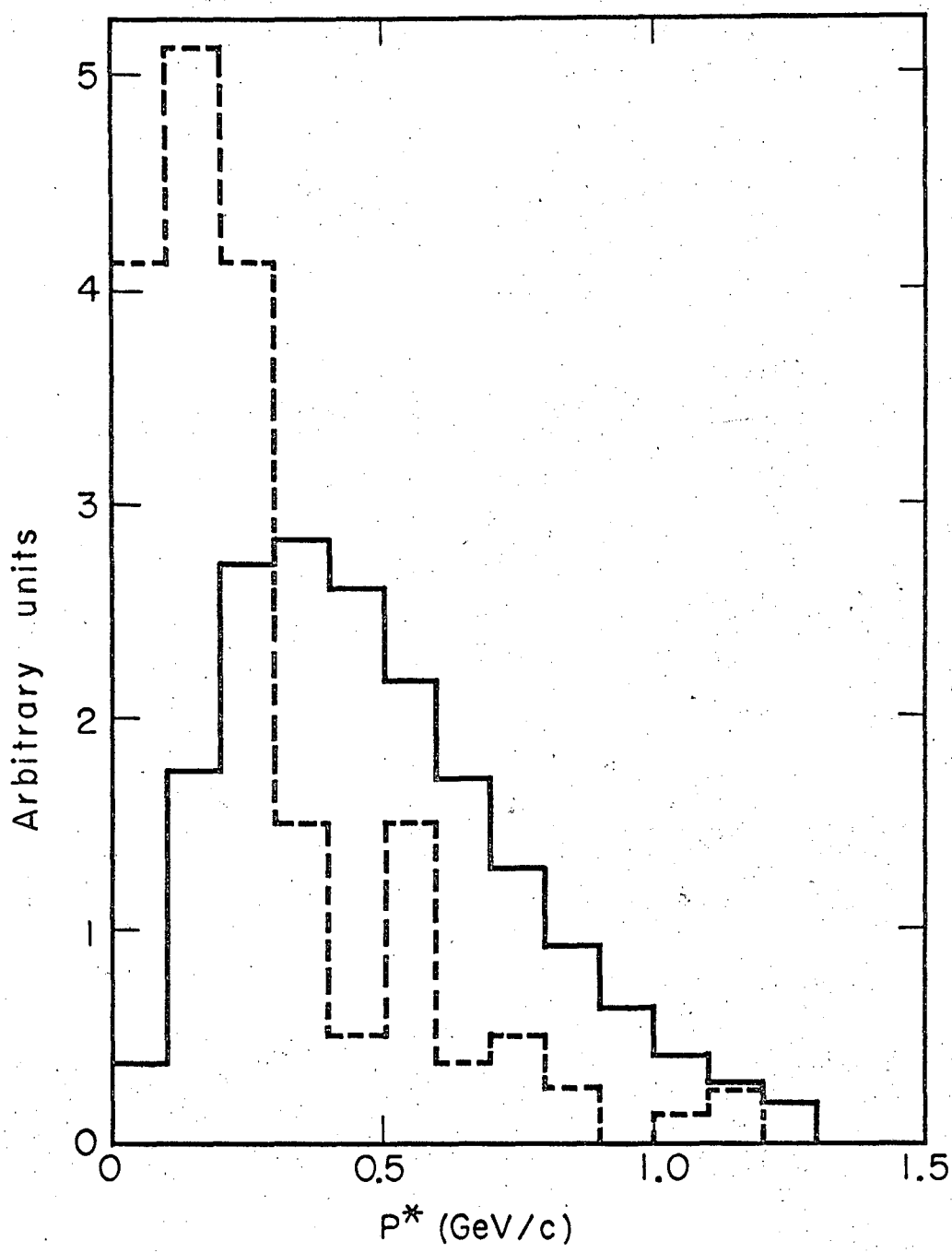

MU-36515

Fig. 7. Pion momentum spectra from 6.2 GeV p - p collisions. Solid histogram is theoretical prediction normalized to the total number of experimental tracks.

The proton momentum spectra is presented in Fig. 8 . It has the same properties with respect to changes in the parameters as the pion spectra. However in this case the theoretical maximum is below the experimental maximum and much sharper. The shape of this curve could probably be improved by variation of the ξ_i individually, but the location of the maximum is very insensitive to these changes. Again this behavior persists at all energies for which data are available.

C. π^-- p Interactions

The analysis of the π^-- p interactions followed the pattern of the p - p analysis. Here we also concentrated upon the energy dependence of the gross features of this reaction and the spectra of emitted particles. The problems encountered were similar to those of the p - p analysis.

1. Gross Features

As in the p - p case the model with all $\xi_i = 1$ predicts too many charged products of the reaction (Fig. 9). If we reduce the ξ - factors of the resonant states, ξ_i^* , to 0.2 we obtain the second curve of Figure 9, which fits the data reasonably well. However any extrapolation in energy for this reaction is subject to the same criticism as for the p - p case. Figures 10 and 11 contain the n_{ch} data and the phase space model predictions for $\xi_i^* = 0.2$. In general the fit to the data is somewhat better in this case than in the p - p case, however the data are not as extensive.

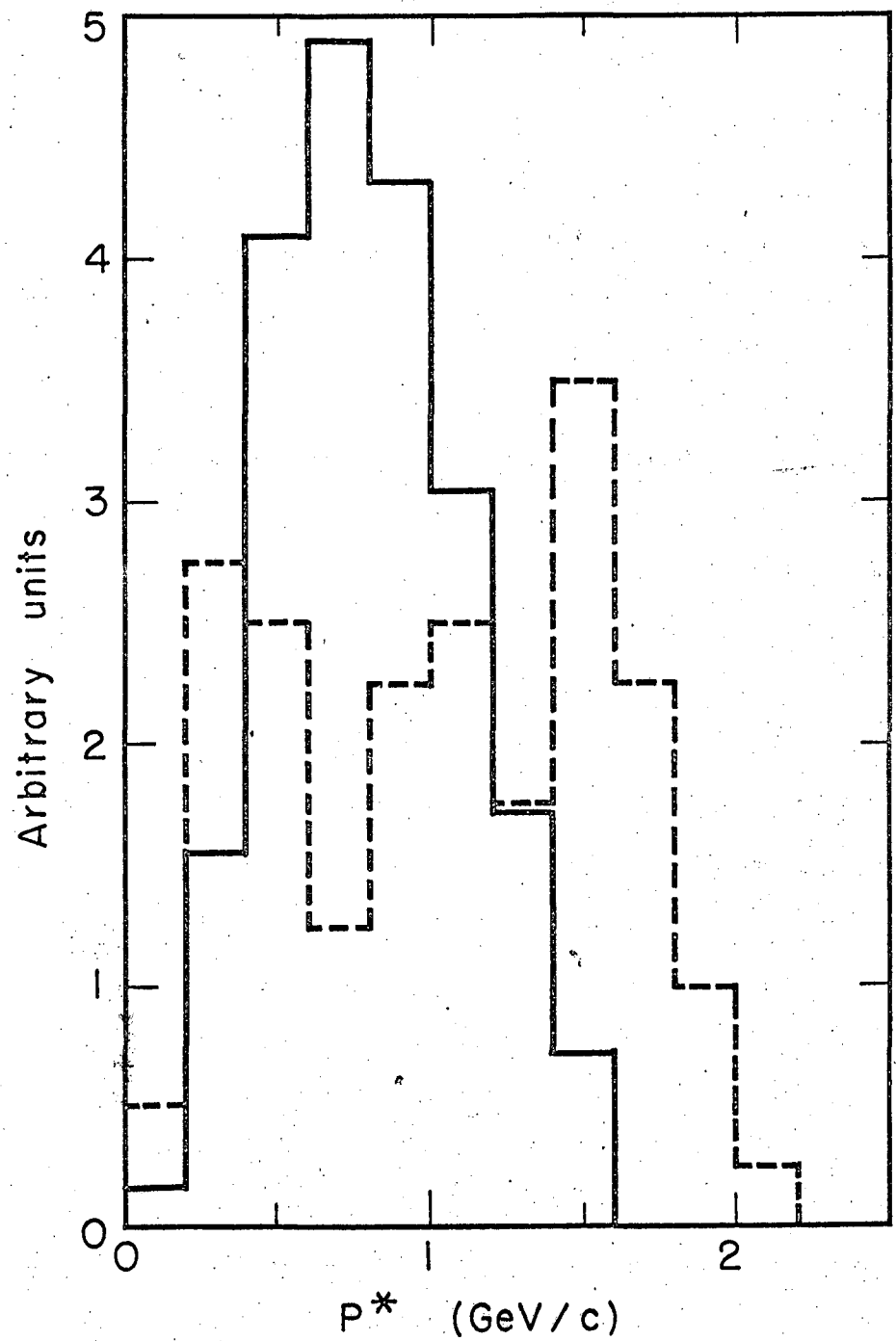

MU-36516

Fig. 8. Proton momentum spectra from 6.2 GeV p - p collisions. Solid histogram is the theoretical prediction normalized to the total number of experimental tracks.

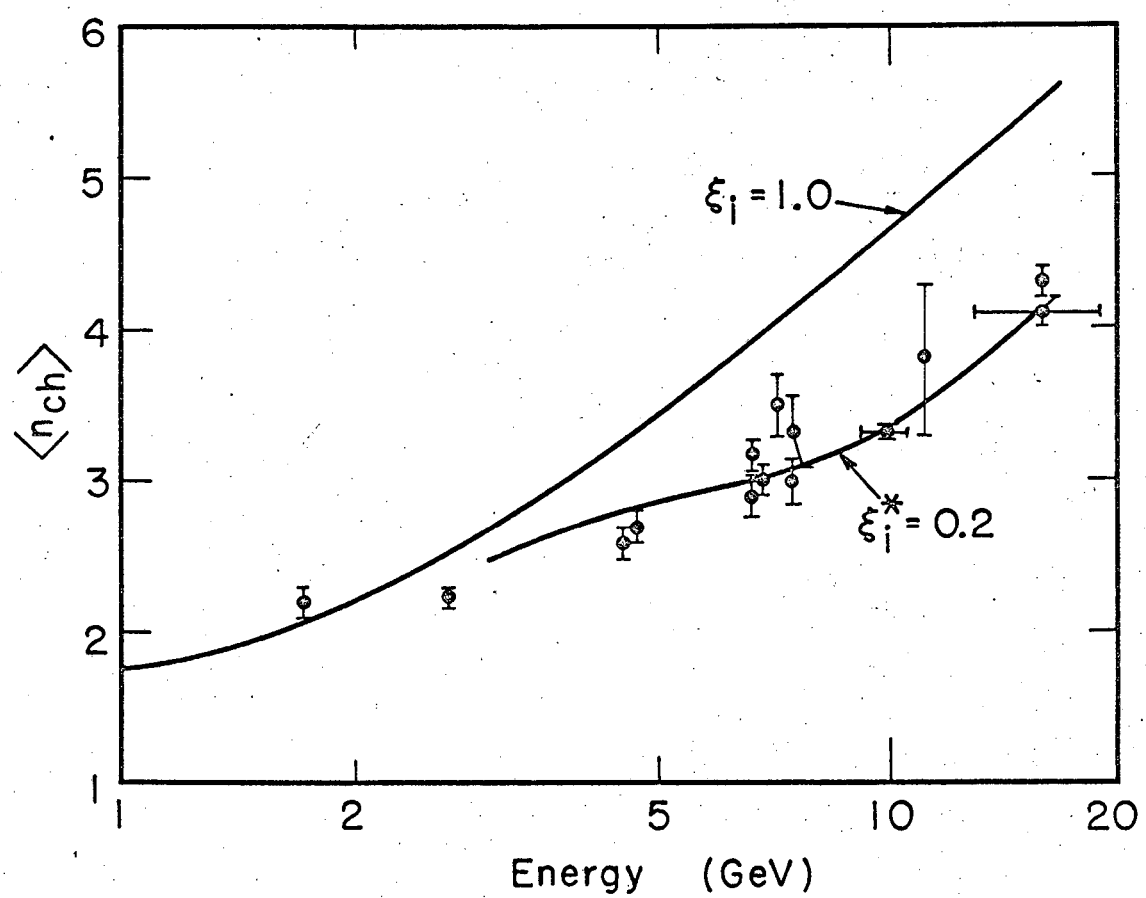

MU-36517

Fig. 9. The variation of $\langle n_{ch} \rangle$ with energy for π^--p collisions.

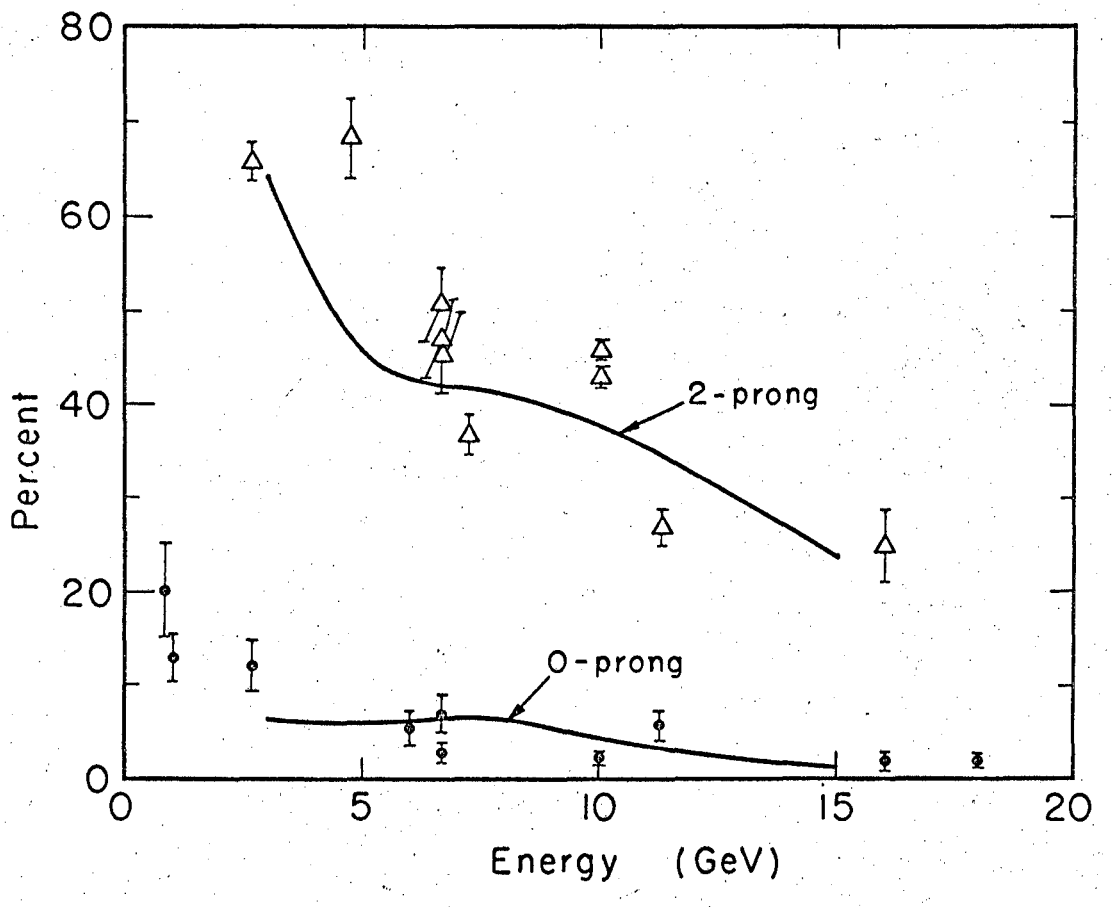

MU-36518

Fig. 10. The variation of the percentage of zero and two prong final states with energy in π^--p collisions. The circles are zero prong data and the triangles are two prong data.

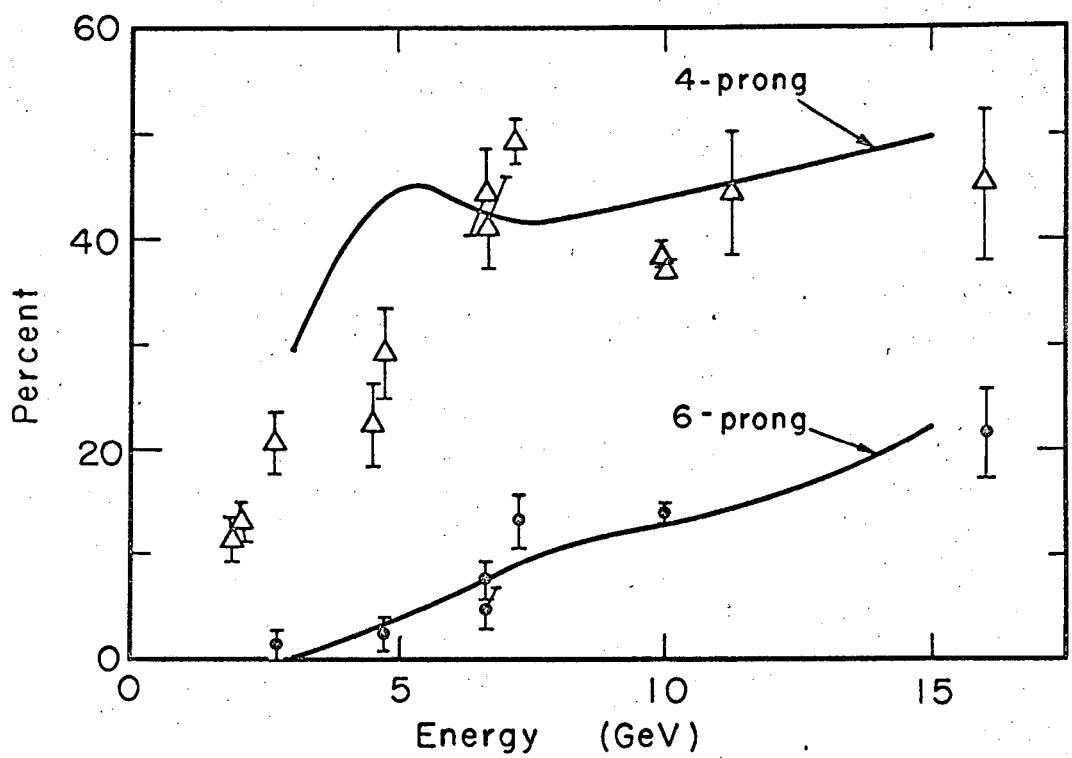

MU-36519

Fig. 11. The variation of the percentage of four and six prong final states with energy in π^--p collisions. The triangles are four prong data and the circles are six prong data.

2. Spectra

We analyzed the spectra produced at 5, 6.8, and 16 GeV incident pion beam energy. We select for discussion the comparison of the results at 6.8 GeV to experiment.[34] The results at other energies were similar to these. Histograms of the experimental data and theoretical predictions for the pion and proton spectra are in Figures 12 and 13 respectively. Here also the fits are somewhat better than in the p - p case, although the fit to the proton spectra is not good. The major failings of the fit to the pion spectra are the peaking at a slightly lower momenta by the theoretical spectrum and a failure to fit the high energy tail of the spectrum. Considering the nature of the model these are not serious difficulties.

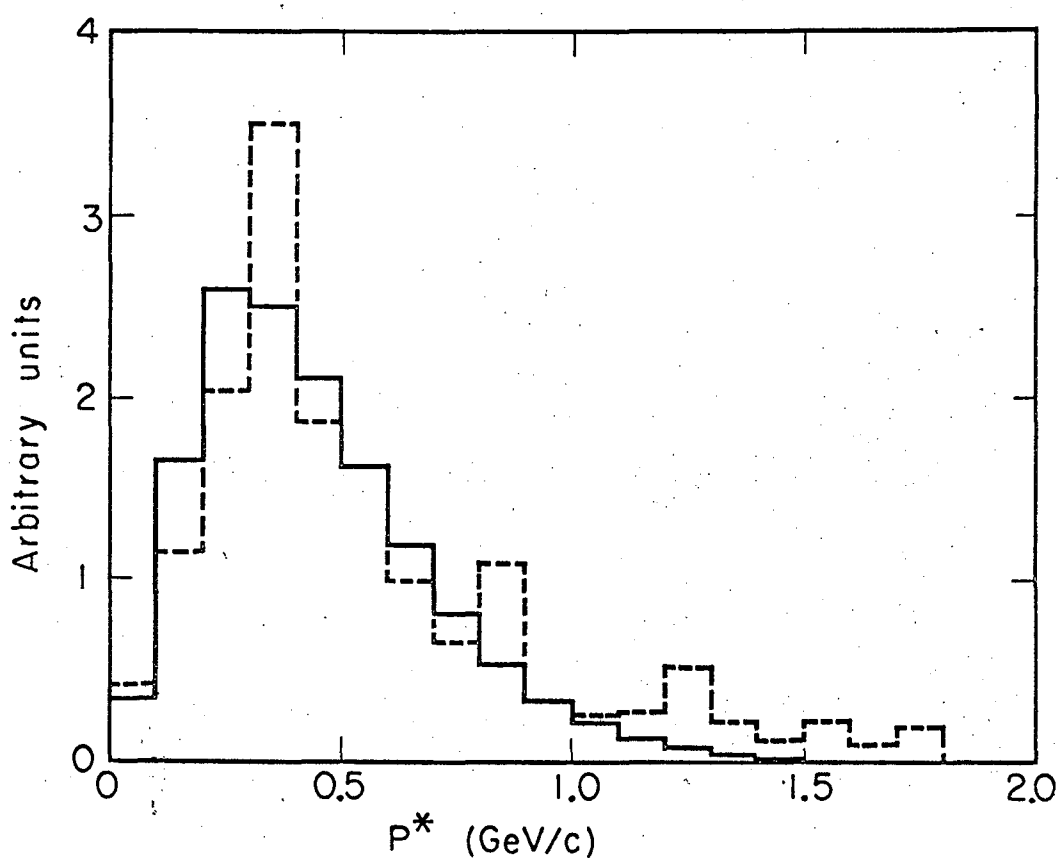

MU-36520

Fig. 12. Pion momentum spectra from 6.8 GeV/c π^--p collisions. Solid histogram is theoretical prediction normalized to the total number of experimental tracks.

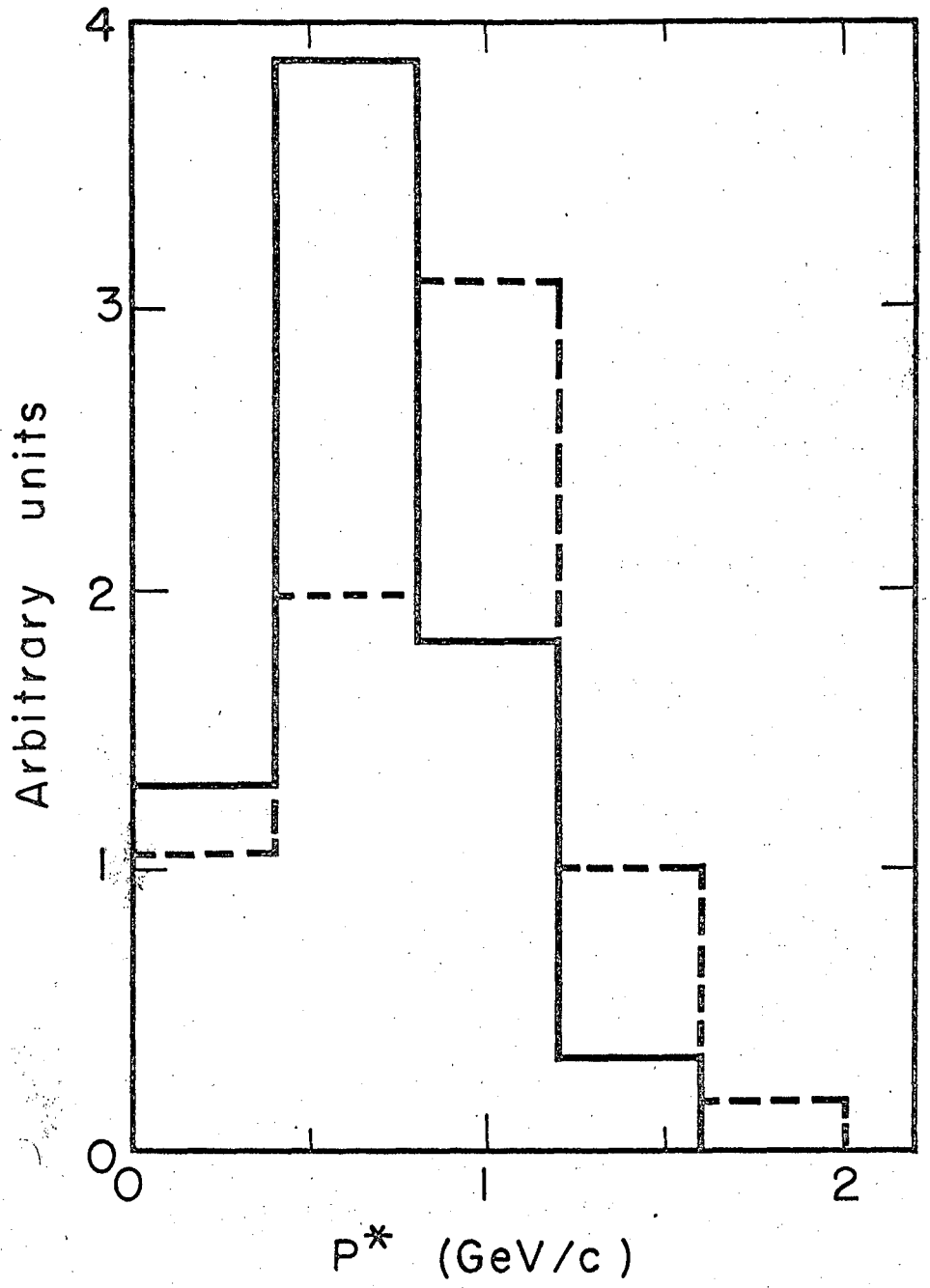

MU-36521

Fig. 13. Proton momentum spectra from 6.8 GeV/c π^--p collisions. Solid histogram is theoretical prediction normalized to the total number of experimental tracks.

VIII. CONCLUSIONS

The phase space model has been used in an attempt to fit the energy dependence of various features of elementary particle reactions. The agreement with experiment for $p - p$ reactions is limited and cannot be expected to persist for higher energies unless an energy dependence is introduced into the volume factors. The fit to the spectra of created particles is poor and we feel that it cannot be improved in a reasonable manner. The situation is better for $\pi^- - p$ reactions, however data are not available for the higher energies where difficulty is expected.

Finally, multiple resonance production is the predominant feature of this model in all reactions, yet this is in contradiction to experiments in $\bar{p} - p$ annihilation. Perhaps experimental evidence on multiple resonance formation in other processes could clarify this situation.

APPENDIX. A. DETAILS OF THE CALCULATION

Two computer programs were used in this calculation. The first did the basic phase space calculation, producing as output various gross features of the reaction such as the average number of various particles produced, the average number and distribution of charged particles, etc. This program also produced the spectra of particles and resonances which the second program used as input. The second program calculated the resultant spectra of long-lived particles and prepared various displays of these spectra (CRT plots, histograms, etc.)

The three basic tasks performed by the first program were the generation of all final states having the appropriate quantum numbers, the calculation of the phase space of these states, and the bookkeeping necessary to prepare the output. The third task presented no problems and was programmed in a straight-forward manner.

In programming the first task we were confronted with the problem that the number of final states allowed by energy conservation increases very rapidly with energy. Care was taken to develop a good criterion for selection of only the important states which would take a minimum of time. The method selected was as follows. Let n_i be the number of particles of the ith type treating all charge states of the particle as a single particle (the sum over various charge

combinations was done at a later point) and not including nucleons, K mesons, or pions in this enumeration. Nucleons were added to a state defined by $\{n_i\}$ to conserve baryon number, K mesons to conserve strangeness, and pions to enable charge to be conserved. The phase space, etc., for this state was then computed and pions were added until the phase space had passed its maximum and fallen below a cutoff percentage (typically 10^{-4}) of the maximum phase space computed previously. If contributing states were found then pairs of K - mesons were added until no such states were found. Then pairs of nucleons were added and the process repeated until no contributing states were found. Then n_0 was increased by one and the process repeated. When no contributing states were found for a given $\{n_i\}$ the n_i were scanned in order of increasing i. The first non-zero n_i found was set to zero unless increasing it would reduce the number of nucleons and K mesons needed to conserve baryon number and strangeness. In the latter case n_i was increased and the new $\{n_i\}$ was used in the above process; in the former case one was added to n_{i+1} and this $\{n_i\}$ was used.

The phase space was evaluated in a straight-forward manner, using Newtonian iteration to locate the saddle point. The necessary Bessel functions were evaluated by a tabular interpolation scheme which employed a variable increment tabulation to retain sufficient accuracy and minimize table sizes. This procedure reduced the running time of the program considerably relatively to that required by an "exact" calculation of the Bessel functions.

The decay spectrum calculation by the second program was conceptually straight forward, however the large number of particles and decay modes required a rather elaborate treatment. The program was structured to utilize data on the decay modes of resonances in tabular form. It was therefore relatively easy to expand or modify. The necessary integrations were performed by the trapezodial rule since this yielded sufficient accuracy.

APPENDIX B. THE NON-COVARIANT PHASE SPACE INTEGRAL

The non-covariant form of the phase space is

$$S_n = \int \delta(E - \sum_{i=1}^{n} \omega_i)\, \delta^{(3)}(\sum_{i=1}^{n} \vec{p}_i) \prod_{i=1}^{n} d^3\vec{p}_i \quad . \qquad \text{(B:1)}$$

This multiple integral may be reduced to a single integral by a method similar to that applied to the covariant form. The resulting integrand is, however, quite complicated and the integral is not as readily approximated.

We start from the expression[35]

$$S_n = \frac{4\pi}{(2\pi)^4} \int_{-\infty - i\epsilon}^{\infty - i\epsilon} d\alpha \int_0^{\infty} d\lambda\, \lambda^2\, e^{i\alpha E} \prod_{k=1}^{n} \left[\frac{2\pi^2 m_k^{\,2}}{\alpha^2 - \lambda^2}\, H_2^{(2)}(m_k \sqrt{\alpha^2 - \lambda^2}) \right] . \qquad \text{(B:2)}$$

The only essential difference between this and the corresponding expression for the covariant phase space is the presence of the factor α^n. Since these integrals define generalized functions we may replace this factor by n-fold differentiation with respect to the energy. Thus

$$S_n = \frac{4\pi}{(2\pi)^4} \left(\frac{d}{dE}\right)^n \int_{-\infty - i\epsilon}^{\infty - i\epsilon} d\alpha \int_0^{\infty} d\lambda\, \lambda^2\, e^{i\alpha E}\, f\left(\sqrt{\alpha^2 - \lambda^2}\right) \qquad \text{(B:3)}$$

where

$$f(\rho) = \prod_{k=1}^{n} \left[\frac{2\pi^2 m_k^{\,2}}{i\,\rho^2}\, H_2^{(2)}(m_k\, \rho) \right] . \qquad \text{(B:4)}$$

Now we use the results of the covariant calculation to obtain

$$S_n = \frac{-i}{(2\pi)^2} \int d\rho\, \rho^2\, f(\rho) \left(\frac{d}{dE}\right)^n \frac{J_1(E\rho)}{E} \quad . \qquad \text{(B:5)}$$

If we let $x = E\rho$, the n-fold derivative may be reduced to polynomials in x^{-1} times $J_o(x)$ and $J_1(x)$. The integral then may, in principle, be approximated by the saddle point technique.

The non-relativistic and ultra-relativistic limits of this form may be investigated by a method analogous to that used for the covariant form. This yields, essentially, the results of Ref. 34.

APPENDIX C. THE NON-RELATIVISTIC PHASE SPACE

The exact form of the phase space using the non-relativistic expression for the energy is well known. However since I have been unable to find a derivation in print, I shall record one here.

The quantity to be calculated is

$$S_n = \frac{d}{dE} \int_D \prod_{i=1}^{n} d^3 p_i \tag{C:1}$$

where D is defined by

$$\sum_{i=1}^{n} \vec{p}_i = 0 \qquad \sum_{i=1}^{n} \frac{|\vec{p}_i|^2}{2m_i} \leqslant E \quad . \tag{C:2}$$

This domain is an ellipsoid in a $3n - 3$ dimensional space and the integral may be evaluated exactly. If we solve the first relation for $\vec{p}_n$ and insert this into the second, we obtain

$$\sum_{i=1}^{n-1} \sum_{j=1}^{n-1} \vec{p}_i \cdot \vec{p}_j \left(1 + \delta_{ij} \frac{m_n}{m_i} \right) \leqslant 2m_n \; E \quad . \tag{C:3}$$

The matrix $B_{ij} = (1 + \delta_{ij} \, m_n / m_i)$ is a real, symmetric matrix, therefore the domain is an ellipsoid. We transform to the principal axis system of the ellipsoid by the orthogonal transformation which diagonalizes B. Let the eigenvalues of B be λ_i and denote the principle axis coordinates by $\vec{\xi}_i$ then

D is now defined by

$$\sum_{i=1}^{n-1} \lambda_i \left|\vec{\xi}_i\right|^2 \leqslant 2\, m_n\, E \quad . \tag{C:5}$$

If we now let $\vec{\eta}_i = \sqrt{\lambda_i}\ \vec{\xi}_i$ we have

$$S_n = \frac{d}{dE}\left(\prod_{i=1}^{n-1} \lambda_i^{-\frac{3}{2}}\right)\int_{D'} \prod_{i=1}^{n-1} d^3\eta_i \quad . \tag{C:6}$$

D' is the interior of a $3n-3$ dimensional sphere of radius $\sqrt{2m_nE}$. In an n-dimensional space the volume of a sphere of radius r is

$$V_n = \frac{\pi^{\frac{n}{2}}}{\Gamma(\frac{n+2}{2})}\, r^n \quad . \tag{C:7}$$

Thus

$$S_n = \left(\prod_{i=1}^{n-1} \lambda_i^{-\frac{3}{2}}\right)\frac{(2\pi)^{\frac{3n-3}{2}}}{\Gamma(\frac{3n-3}{2})}\, m_n^{\frac{3n-3}{2}}\, E^{\frac{3n-5}{2}} \quad . \tag{C:8}$$

The product of the λ_i is the determinant of B which can be shown to be

$$\left(\prod_{i=1}^{n-2} \alpha_i\right)\left[1 + \alpha_{n-1} + \alpha_{n-1}\left(\frac{1}{\alpha_1} + \frac{1}{\alpha_2} + \cdots + \frac{1}{\alpha_{n-2}}\right)\right] \tag{C:9}$$

where $\alpha_i = m_n/m_i$. Thus

$$\frac{m_n^{\frac{3n-3}{2}}}{\left[\prod_{i=1}^{n-1} \lambda_i\right]^{\frac{3}{2}}} = \left[\frac{\prod_{i=1}^{n} m_i}{\sum_{i=1}^{n} m_i}\right]^{\frac{3}{2}} \tag{C:10}$$

and

$$S_n = \frac{(2\pi)^{\frac{3n-3}{2}}}{\Gamma(\frac{3n-3}{2})} \left[\frac{\prod_{i=1}^{n} m_i}{\sum_{i=1}^{n} m_i}\right]^{\frac{3}{2}} . \tag{C:11}$$

To compare this result to the non-relativistic limit of the covariant phase space we must recall the covariant phase space has extra factors of ω_i^{-1} in its definition, which become m_i^{-1} in the non-relativisitic limit.

FOOTNOTES AND REFERENCES

1. Enrico Fermi, Progr. Theoret. Phys. (Japan) 5, 570 (1950).
2. R. Hagedorn, Nuovo Cimento 15, 434 (1960).
3. We use units such that $\hbar = c = 1$ and a metric with signature $(+---)$.
4. F. Cerulus, Nuovo Cimento 22, 958 (1961).
5. The present calculation takes $\sim$ 2 minutes on an IBM 7094 for 15 GeV incident particles. Since an equivalent calculation for each partial wave would be required and about 50 partial waves would be necessary the calculation would be on the borderline of practicality. However, the present method of calculation would be inapplicable and a Monte-Carlo evaluation of the phase space would take at least an order of magnitude longer.
6. S. Z. Belen'kii and A. I. Nikishov, JETP 28, 744 (1955) (Russian); Soviet Physics - JETP 1, 593 (1955) (English translation)
7. S. Z. Belenky, Nuc. Phys. 2, 259 (1956 and 1957).
8. Note that for plane waves

$$\int_{\Omega} \psi^* \psi \, d^3r = \frac{\Omega}{V} .$$

Thus $\left(\frac{\Omega}{V}\right)^{n-1}$ is the probability of finding all n particles in the volume Ω . The power is $n-1$ since the volume Ω may be anywhere in V.

9. H. P. Stapp, Phys. Rev. 125, 2139 (1962).

10. In Stapp's notation (Ref. 8) the unitarity relation reads

$$M(K', -\tilde{K}'') + M^*(K'', -K') = -\sum_{\tilde{K}}^{\rho} M(K', -\tilde{K})\, K \cdot \tilde{\sigma}\, M^*(K'', -\tilde{K}) .$$

The term $K \cdot \tilde{\sigma}$ in the integral is essentially the energy dependent factor due to spin that should be included in the phase space integral.

11. This may be justified by considering the δ-function to be the derivative of a unit step function of the energy $\theta(E-q)$ which has the representation

$$\theta(E-q) = \frac{1}{2\pi i} \int_{-\infty - i\epsilon}^{\infty - i\epsilon} \frac{dt}{t} \left[e^{i(E-q)t} - e^{-iqt} \right] .$$

12. G. N. Watson, Theory of Bessel Functions (Second Edition) p. 180.
13. S. Bochner and K. Chandrasekharan, Fourier Transforms (Princeton University Press, Princeton, 1949) p. 69.
14. Watson - op. cit. p.167.
15. Watson - op. cit. p. 172.
16. Watson - op. cit. p. 78.
17. Watson - op. cit. p. 75.
18. This may be demonstrated by computing the logarithmic derivative of $g(\rho)$ and inserting asymptotic forms of the Bessel functions.
19. Watson - op. cit. p. 198. The symbols (ν, m) are defined there.
20. E. T. Whittaker and G. N. Watson, A Course of Modern Analysis, (Fourth Edition) p. 245.

21. Watson - op. cit. p. 15.

22. Eugene P. Wigner, Group Theory and Its Application to the Quantum Mechanics of Atomic Spectra (Academic Press, New York and London, 1959) p. 118.

23. Wigner - op. cit. p. 167.

24. Since this work was originally completed a remarkably similar treatment has been published by R. Hagedorn, Relativistic Kinematics (W. A. Benjamin Inc., New York, 1964) Chapt. 7.

25. See Martin Kretzschmar, Statistical Methods in High-Energy Physics, Ann. Rev. of Nuc. Sci., Vol. 11, p. 1 (1961) for a review. The experimental data used for comparison is from the work of M. Cresti et al. Aix-en-Provence Conference on Elementary Particles, Vol. I, p. 269 (1961), and Proceedings of the Sierra International Conference on Elementary Particles (1963) p. 263.

26. Theodore E. Kalogeropoulos, A Study of The Antiproton Annihilation Process in Complex Nuclei (Ph.D. Thesis) UCRL-8677, March, 1959.

27. T. F. Hoang, Note on the Analysis of K-meson Production By $\bar{p}$ Annihilation, UCRL-8994 Rev. Nov. 1960.

28. H. Satz, The High Energy Limit of the Statistical Model, preprint of Summer Institute for Theoretical Physics, University of Wisconsin, Madison, Wisconsin .

29. The experimental data are taken from Barashenkov V. S., Maltsev V.M., Patera I., Inelastic Interactions of Particles at High Energies, P-1577 Joint Institute for Nuclear Research, Dubna (1964).

30. Considering this data and the data on the average number of charged pions (which is not presented) a somewhat better overall fit to this data is obtained for $\xi_i^* = .10$. This degrades the fit to $\langle n_{ch} \rangle$ somewhat and does not change any of the conclusions.

31. A trivial extension of the results of Ref. 27 gives for the asymptotic dispersion

$$\Delta n = \sqrt{\overline{n^2} - \overline{n}^2} = \frac{1}{\sqrt{3\,\overline{n}}} .$$

32. P. M. Kalbach, J. J. Lord, C. H. Tsao, Phys. Rev. 113, 330 (1959).

33. For $\xi_i^* = .05$.

34. V. A. Belyakov et al, Soviet Physics - JETP 12, 650 (1961).

35. Joseph V. Lepore and Richard N. Stuart, Phys. Rev. 94, 1724 (1954).

ACKNOWLEDGMENTS

I would like to express my deep appreciation to Joseph V. Lepore and Robert J. Riddell who provided the initial impetus for this work and whose continuing advice and encouragement made its completion possible.

This report was prepared as an account of Government sponsored work. Neither the United States, nor the Commission, nor any person acting on behalf of the Commission:

A. Makes any warranty or representation, expressed or implied, with respect to the accuracy, completeness, or usefulness of the information contained in this report, or that the use of any information, apparatus, method, or process disclosed in this report may not infringe privately owned rights; or

B. Assumes any liabilities with respect to the use of, or for damages resulting from the use of any information, apparatus, method, or process disclosed in this report.

As used in the above, "person acting on behalf of the Commission" includes any employee or contractor of the Commission, or employee of such contractor, to the extent that such employee or contractor of the Commission, or employee of such contractor prepares, disseminates, or provides access to, any information pursuant to his employment or contract with the Commission, or his employment with such contractor.